45P

FACILITY FORM 602
N65-88681 (ACCESSION NUMBER)
45 (PAGES)
TMX-52488 (NASA CR OR TMX OR AD NUMBER)
(THRU)
(CODE)
(CATEGORY)

NOTCH EFFECTS ON FATIGUE AND STATIC STRENGTH

By Paul Kuhn

NASA Langley Research Center
Langley Station, Hampton, Va., U.S.A.

Presented at the Symposium on Aeronautical Fatigue
Sponsored by the International Committee on Aeronautical Fatigue (ICAF)
and the Structures and Materials Panel of the Advisory Group for
Aeronautical Research and Development (AGARD)

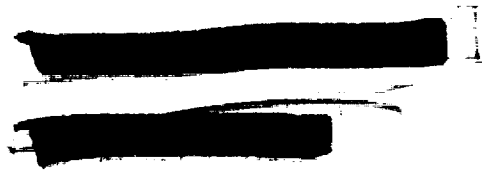

Rome, Italy
April 1963

NATIONAL AERONAUTICS AND
SPACE ADMINISTRATION
WASHINGTON

Code 2a

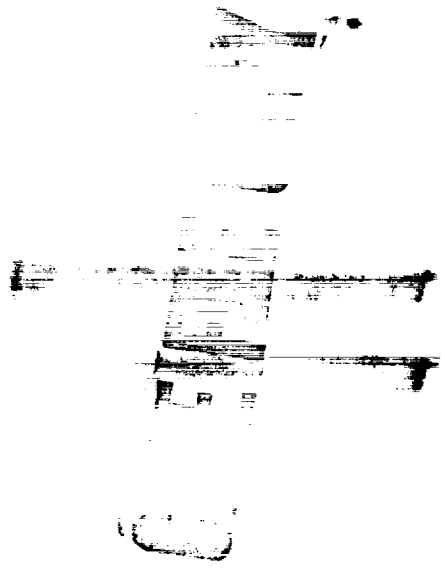

TABLE OF CONTENTS

	Page
SUMMARY	1
INTRODUCTION	1
SYMBOLS	3
METHOD OF NOTCH ANALYSIS	4
Formulas for Analysis	4
General Remarks on the Neuber Constant	7
Determination of the Neuber Constant	7
APPLICATIONS TO CLASSES OF MATERIALS	9
Fatigue Notch Strength of Low-Alloy Steels	9
Fatigue and Static Notch Strength of Wrought Aluminum Alloys	10
Static Notch Strength of Titanium Alloys	12
Rate of Propagation of Fatigue Cracks	13
SPECIAL APPLICATIONS	13
Correlation of Results From Different Types of Specimens	13
Criteria for Comparison of Materials	15
CONCLUDING REMARKS	17
APPENDIX	19
Buckling Correction	19
Curvature Correction	19
REFERENCES	20
TABLE I	21
FIGURES	22

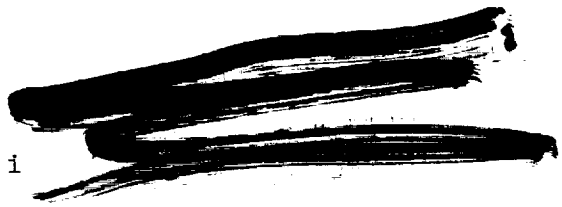

NOTCH EFFECTS ON FATIGUE AND STATIC STRENGTH

by

Paul Kuhn*

SUMMARY

13181

Tensile stresses in structural components cause failure, as a rule, at some geometric discontinuity. Engineering predictions of such failures require the development of methods which take into account realistically the complex interplay between stress distribution and material's behavior. This paper gives a status report on a method originally formulated to deal with the fatigue notch strength of low-alloy steels, then applied to the fatigue and static notch strength of aluminum alloys, and now extended to cover the static notch strength of titanium alloys at temperatures ranging from cryogenic to moderately elevated. In the discussions of static notch strength, attention is focused mostly on the problem of parts containing cracks, a problem which has been of vital interest for years in several fields of engineering. The method is also useful for correlating data on the rate of propagation of fatigue cracks.

INTRODUCTION

Notches appear in profusion in any practical structure or machine. Some well-known examples appear in figures 1(a), (b), and (c): a groove in a shaft, a shoulder or abrupt change of cross section, and a circular hole. The Vee-notch (fig. 1(d)) probably does not appear very often in practical structures, but it is the outstanding favorite for purposes of engineering research. The effect of a notch on the strength of a part can be defined by a stress-concentration factor; different factors must be used, however, for static strength and for fatigue strength. The goal of engineering research is the ability to predict these factors with a minimum of special information or testing.

An extreme form of a notch is a crack. Cracks can result from fatigue loading, from thermal stresses - especially welding - or from mechanical damage in service. In the past, it has not been necessary to deal with cracks quantitatively. However, airworthiness regulations now call for proof that structures containing cracks of stipulated length can carry a stipulated fraction of the design ultimate load. Methods of calculations are highly desirable, because the cost of giving the required proof by test is extremely high for large structures such as airplane fuselages.

The need for dealing with the strength of cracked parts brings about the need for information on another subject: the rate at which fatigue cracks propagate under the repeated loads sustained in service. This information is needed

---

*Assistant Chief, Structures Research Division.

in order to estimate whether a crack will propagate to a catastrophic length within one inspection period.

The problem of notch effects in its full generality, as outlined above, is a complex one. Historically, its solution has been approached in gradual stages.

In the first stage, notch problems in static-strength design were in effect avoided by using very ductile materials. This simple approach gradually became inadequate, partly because it was discovered that some materials tend to lose their ductility at low temperatures, partly because metallurgical developments resulted in materials of higher strength, but with less ductility. At this stage, it was also discovered that elongation by itself is not an adequate measure of such manifestations of ductility as result in serviceability of structures. A search was therefore begun for special tests which would permit the comparative ranking of materials, and this search is continuing to this day.

Tremendous amounts of money and time have been spent in the last two decades on this line of approach, and it has been eminently useful in some fields of engineering. In particular, the ranking tests have been invaluable tools for improving the production control and the processing of materials. However, these tests are not sufficiently quantitative to be useful either in design or in strength analysis in fields where close control of weight and strength is imperative, as in the design of aircraft or space structures. In fact, the majority are of such a nature that it is almost impossible to conceive any application to a routine strength-analysis problem. On the other hand, designers in many fields have been for years under ever-increasing pressure to improve their methods of strength analysis and design. A quantitative method of notch analysis is thus becoming a necessity.

Parallel to the problem of static-strength design is that of fatigue design. Here, it became clear very early that notch effects are so important that they can very seldom be disregarded with impunity. Attempts to deal quantitatively with notches under fatigue loading consequently began much earlier and have been carried much farther than for static loading. Little or no connection existed for a long time between the two lines of effort.

The present paper gives a review and a status report on a method originally formulated to deal with the fatigue notch strength of low-alloy steels (ref. 1) and expanded into a unified method for dealing with static as well as fatigue notch analysis of aluminum alloys (ref. 2). The method has recently been expanded further by applying it to the static notch-analysis of titanium alloys at temperatures ranging from cryogenic to moderately elevated, and of aluminum alloys at cryogenic temperatures.

The paper presents first the formulas and curves which comprise the method. Next, sample applications to all materials are shown. The correlation of rates of fatigue-crack propagation is discussed briefly. The last part of the paper illustrates suggested uses of the method for the purpose of correlating the notch tests currently performed on a large variety of specimen types and suggests quantities that may be used for the purpose at comparing materials.

SYMBOLS

A_N	area of net section, sq in.
a	half-length of transverse slot or crack, or depth of edge notch or crack, in. (Note: Crack length used is initial value, measured before load is applied.)
B	flow-restraint parameter defined by figure 3
E	modulus of elasticity, ksi
E_1	secant modulus of elasticity pertaining to tensile ultimate stress, ksi
e	elongation in 2-inch gage length, in./in.
K_c	fracture-mechanics quantity, ksi $\sqrt{\text{in.}}$
K_F	stress-concentration factor effective in fatigue (experimentally obtained)
K_N	stress-concentration factor corrected for size effect (Neuber factor); also predicted value of stress-concentration factor effective in fatigue near fatigue limit (fully reversed loading)
K_P	value of K_N corrected for plasticity effect
K_T	theoretical stress-concentration factor
K_{TN}	asymptotic limit of K_N as $\rho \to 0$
K_u	static notch (strength) factor
K_u^*	static notch (strength) factor corrected for flow restraint (see formula (1d))
K_w	factor providing for finite width of part, given by figure 4
R	radius of cylinder, in.
S_N	average stress on net section at failing (maximum) load, ksi
t	thickness of specimen, in.
w	width of specimen, in.
ρ	radius of notch, in.
ρ'	material constant (Neuber constant), in.

σ_u tensile ultimate strength, ksi

σ_{ty} tensile yield strength, ksi

ω flank angle of notch, radians (fig. 2)

ω_e effective flank angle (for use in formula (3))

METHOD OF NOTCH ANALYSIS

Formulas for Analysis

In the present paper, attention is focused mainly on the problem of the static notch strength of sheet-metal parts under axial load (fig. 2.) More extensive discussions, particularly of fatigue problems, may be found in references 1 and 2. With some minor changes, the presentation of the formulas here follows reference 2.

The average stress in the net section of a notched part will be denoted herein by $S_N(=P/A_N)$. The peak stress in the net section, which occurs at the bottom of the notch, may be expressed as the product of S_N and of a factor of stress concentration. Failure of the part is presumed to take place when the peak stress becomes equal to the strength of the material. Thus, the criteria for failure may be written as

$$S_N K_u = \sigma_u \quad \text{for static strength of a part with a crack} \tag{1a}$$

$$S_N K_u^* = \sigma_u \quad \text{for static strength of a part with a notch} \tag{1b}$$

$$S_N K_N = \sigma_F \quad \text{for fatigue strength of a part with a notch} \tag{1c}$$

In these expressions, σ_u is the tensile strength of the material, and σ_F is the fatigue strength for the stipulated number of load cycles. Calculation of the stress-concentration factors K_u, K_u^*, and K_N constitutes the objective of the method of notch analysis.

The distinction between parts with cracks and parts with (finite-radius) notches is necessary because the latter exhibit "notch-strengthening" effects as a result of flow restraint (ref. 2); the ultimate strength is thus increased. For convenience in routine analysis, however, rather than multiplying σ_u by a factor $(1 + B)$, the factor K_u is divided by $(1 + B)$ to obtain

$$K_u^* = \frac{K_u}{1 + B} \quad (B \text{ from fig. 3}) \tag{1d}$$

The use of K_u^* permits listing a single number (σ_u) as "allowable stress" in manuals. (In the expression for K_u^* given in reference 2, the quantity B appears with two correction factors. These factors have been omitted here because currently available experimental evidence is not considered adequate to justify their use.)

The process of computing the desired factor of stress concentration begins with obtaining the appropriate theoretical factor K_T by the theory of elasticity or equivalent means, such as photoelastic tests. For the configurations shown in figure 2, which cover the cases of greatest interest for this paper, the formula

$$K_T = 1 + 2K_w\sqrt{\frac{a}{\rho}} \qquad (K_w \text{ from fig. 4}) \tag{2}$$

is used. This formula is rigorously correct only for an elliptical hole in an infinitely wide sheet (with $K_w = 1$), but is the best available basis for the following steps. The dashed curves in figure 4 are based on photoelastic tests of specimens with U-notches or slots (ref. 3); the full-line curve is computed from the analytical expression indicated in the figure.

In the next step, K_T is corrected for the "size effect" which is exhibited by materials with granular structure when stress gradients are present (refs. 1 and 2). The corrected factor, denoted K_N, is obtained by use of the formula

$$K_N = 1 + \frac{K_T - 1}{1 + \frac{\pi}{\pi - \omega_e}\sqrt{\frac{\rho'}{\rho}}} \tag{3}$$

where $\omega_e = \frac{1}{2}\omega$ for $\omega < 2$ radians.

The quantity ρ' is termed "Neuber constant" and is presumed to be a materials constant; it will be discussed in the following section.

In the third step, K_N is written for the effect of plasticity by means of the general formula

$$K_P = 1 + \left(K_N - 1\right)\frac{E_1}{E} \qquad \left(S_N < \sigma_{ty}\right) \tag{4}$$

where E is Young's modulus and E_1 is the secant modulus pertaining to the peak stress at the root of the notch. (Cases for which $S_N > t_y$ are discussed in ref. 2.) By inserting the appropriate value of E_1 in formula (4), the special value of K_P valid at failure (either fatigue or static, as desired) is obtained.

In this paper, consideration will be given only to fatigue failures near the fatigue limit. In such cases the peak stress is in the plastic range. Thus, $E_1 = E$ and formula (4) takes the specialized form

$$K_P = K_N \tag{5}$$

signifying that the factor K_N given by formula (3) constitutes the predicted value of the fatigue notch-strength factor for fully reversed loading near the fatigue limit.

If the static notch-strength factor is desired, it is necessary to insert into formula (4) for E_1 the secant modulus associated with σ_u, the maximum stress carried by a standard tensile specimen. The complete stress-strain curve necessary to derive this modulus is seldom available. However, the elongation e (measured after fracture) is measured in most tensile tests and is included in the information conventionally furnished by the materials producer. Consequently, for the analysis of tests on aluminum alloys reported in reference 2, the following procedure was adopted for an approximate determination of the ratio E_1/E.

Complete stress-strain curves were obtained for a number of specimens of 2024-T3, 2024-T4, and 7075-T6 alloy, and the elongations e were also measured after fracture. The average ratio of (permanent) elongation at maximum load to final permanent elongation was determined from these tests and found to be 0.8. It was then assumed that this ratio is applicable to all other aluminum alloys. With this assumption, and taking into account the elastic elongation,

$$\frac{E_1}{E} \approx \frac{1}{1 + \frac{0.8eE}{\sigma_u}} \tag{6}$$

with the elongation e measured on the standard 2-inch gage length. In the present paper, this formula has also been applied to titanium alloys. Obviously, the assumption of a constant factor of 0.8 for all materials is only a first approximation, but it is believed that other uncertainties in the presently available test data overshadow the effect of this assumption in most cases.

For <u>cracks</u>, the tip radius ρ is indefinitely small; thus, K_T is indefinitely large and useless. However, for these conditions ($\rho' \gg \rho$; $\omega = 0$), the factor K_N assumes a limiting value, denoted K_{TN}, which is obtained by combining formulas (2) and (3) as

$$K_{TN} = 1 + 2K_w \sqrt{\frac{a}{\rho'}} \tag{7}$$

Formula (4) is then used to obtain K_u using K_{TN} instead of K_N.

General Remarks on the Neuber Constant

The Neuber constant ρ' must be regarded as a mathematical device used in the process of converting K_T factors, which are valid only for homogeneous materials in the elastic range, into factors which define failure, either fatigue or static. From this definition, it follows that ρ' has no meaning when dissociated from the formulas in which it appears; at least, no such meaning has been clearly defined so far. As a corollary, it is meaningless, in general, to compare ρ' - values derived by different investigators using different sets of formulas, and it is not permissible, in general, to use ρ' - values given by one investigator in conjunction with formulas given by another investigator.

Values of ρ' can be derived either from notch fatigue tests or from static tests on notched or cracked parts. The constant ρ', in effect, furnishes a phenomenological description of some failure characteristics of the material. Now, it is generally believed that the mechanism of failure under fatigue loading differs from that under static loading. Thus, it might be concluded, a priori, that ρ' values derived from fatigue tests would not be identical with values derived from static tests.

However, this a-priori conclusion has been disproved for wrought aluminum alloys in reference 2, where it was shown that the same ρ' values can be used to predict static as well as fatigue notch strengths. With this precedent, it may be hoped that the same fortunate situation will exist for other materials, but test data available at present are completely inadequate to prove or disprove this hope.

For low-alloy steels, the method has been applied only to the analysis of notch-fatigue tests (ref. 1). This application was made chiefly because the literature contained a vast amount of test data that could be used for initial verification of the method. No attempt has been made to investigate the static strength of low-alloy steel parts with sharp notches, largely because this problem has not been of sufficient interest for aeronautical applications.

Titanium alloys, on the other hand, are of great interest for aeronautical use; consequently the applicability of the method to such alloys has been investigated recently. Because of the great interest in the problem of static notch sensitivity that has developed in the past few years, a rather large amount of static notch-test information is available considering the fact that titanium technology is still in a state of rapid development. On the other hand, notch-fatigue data on titanium are still rather scarce; a brief preliminary analysis of these data disclosed such a "shotgun pattern" of results that there appears to be no hope of developing a prediction method for notch-fatigue factors applicable to titanium alloys until a reasonable amount of much more reliable test data becomes available.

Determination of the Neuber Constant

For low-alloy steels (defined for this purpose as having Fe > 90 percent), Neuber constants have been determined from notch-fatigue tests (ref. 1). It was

found that they could be represented as a function of the tensile strength of the material, and the resulting curve is reproduced in figure 5(a).

A similar analysis for aluminum alloys (ref. 2) resulted in two curves, reproduced here in figure 5(b), one for heat-treated materials and one for annealed or strain-hardened materials. These curves are derived from fatigue tests, but are applicable to notch fatigue as well as static notch strength.

Figure 5(c) shows recently derived curves for titanium alloys, based on static notch tests. These curves should be regarded as tentative, because some test results show sharp differences for nominally identical materials between different laboratories and even within one laboratory.

The curve in figure 5(a) for low-alloy steel is based on room-temperature tests. The curves in figure 5(b) for aluminum alloys were originally based on the analysis of room-temperature tests, but have been applied to tests at cryogenic temperatures (to -320° F), as will be shown later, without loss of accuracy of prediction. The curves for titanium alloys (fig. 5(c)) have been used for the temperature range from -420° to +800° F; again, the scatter appears to be no worse than at room temperature. It should be noted that tensile strengths higher than about 220 ksi on titanium alloys have been attained to date only at cryogenic temperatures.

For materials not covered by the curves shown in figure 5, individual determinations of ρ' must be made. Depending on the intended use, either notch-fatigue tests or static notch tests may be made.

Fatigue tests involve the determination of the unnotched fatigue strength and of the notched fatigue strength for some chosen notch configuration. As is well known, scatter in fatigue tests results in the need for a fair number of specimens if reasonable accuracy is to be obtained. With regard to notch configuration, a compromise must be made, particularly if rotating beams are used. A large notch radius affords good accuracy of radius measurement and also good control of surface finish. On the other hand, it results generally in a fatigue factor K_F close to unity, say 1.20 ± 0.05. Now, the calculation of ρ' is based on the quantity $(K_F - 1)$, or in this example (0.20 ± 0.05): thus, the test uncertainty (± 0.05) looms large in comparison with the test quantity 0.20. If an attempt is made to improve the ratio of test quantity to test uncertainty by using a significantly higher value of K_F, a much smaller radius must be used. This reduces the accuracy of radius measurement, reduces the control of surface finish in the notch, and greatly increases the danger of setting up residual stresses at the bottom of the notch which may affect the result to such an extent that the test is useless for determining ρ'. Thus, an intermediate value of notch radius is probably the best compromise. The determination of ρ' involves only formula (3); thus, no material properties other than the two fatigue strengths need be known, which is a useful fact.

The determination of ρ' from static tests is done best (for sheet material) with specimens containing central fatigue cracks (fig. 2(d)). The specimen should be wide enough to fail at a net-section stress no greater than the yield stress and should be as wide as practicable in order to make the quantity $(K_u - 1)$ as

large as possible (a proposed semistandard width is 8 inches). Several crack lengths (preferably from 20 to 50 percent of specimen width) should be used to obtain some idea of scatter. The evaluation of ρ' involves the use of expressions (4), (6), and (7); thus, the material properties E, e, and σ_u must be known. The largest inaccuracy usually results from statistically inadequate values of the elongation e.

The determination of ρ' from static tests on specimens with finite-radius notches requires knowledge of the flow-restraint parameter B appearing in expression (1d). Curves for this parameter are currently available only for aluminum and titanium alloys (fig. 3), and these curves are only rough approximations. Trial calculations show quickly that specimens with mild notches cannot be used because of this uncertainty on B; the use of very sharp notches is imperative. On aluminum alloys, notches with a radius of 0.005 inch have been used with fair success. Radii of this magnitude can be produced economically and fairly accurately by drawing nylon threads impregnated with abrasive in a reciprocating motion over the end of a fine saw cut. Radii less than 0.001 inch have been used to a considerable extent, but the accuracy of radius measurement is quite poor, and the effort needed to produce such radii under reasonable control is so large that it would seem much more practical to go to the limit and use fatigue cracks in preference to radii less than 0.005 inch.

The concept of a Neuber constant becomes obviously questionable when the material properties vary significantly through the thickness. However, clad aluminum-alloy sheets containing cracks have been analyzed with good success by computing K_u for the core material and then using the tensile strength σ_u of the combination (core plus cladding) when computing the net-section stress carried at failure. For steel with decarburized skin, on the other hand, properties may be drastically different and ad-hoc tests are then necessary (ref. 4).

APPLICATIONS TO CLASSES OF MATERIALS

Fatigue Notch Strength of Low-Alloy Steels

Some typical comparisons between experimental and predicted fatigue notch factors for parts made from low-alloy steels are shown in figures 6 and 7. These test sets have been chosen from reference 1 because they demonstrate the size effect graphically. Figure 6 shows results for shafts of varying diameter with grooves either geometrically similar or of fixed size. The agreement between experimental points and predicted values (dashed curves) is excellent. Figure 7 shows results for geometrically similar series of shafts with filleted shoulders. Here, the agreement between test and prediction is excellent for two series, but one series shows a consistent discrepancy. The magnitude of the discrepancy - about 10 percent - is typical of what should be expected in many cases due to limitations of either the method or the test data. Discussions of possible reasons for discrepancies other than weakness of the method of prediction may be found in references 1 and 2. Table I(a) gives an indication of the accuracy of prediction achieved for the tests analyzed in reference 1.

Fatigue and Static Notch Strength of Wrought Aluminum Alloys

The analysis of a collection of notch-fatigue data for aluminum alloys is given in reference 2. The data are less extensive and cover a much smaller variety of configurations than for the low-alloy steels. The over-all scatter is somewhat greater than for steel. In particular, there is in some cases a rather disconcertingly large scatter and lack of agreement between laboratories for nominally identical tests on the highest-strength (zinc) alloy tested. In one case, a test series on rotating beams with grooves was duplicated in another laboratory in an attempt to obtain more consistent results. However, the consistency was not improved, and differences between the two laboratories were as high as 30 percent for the fatigue strengths and as high as 50 percent for the fatigue factors. In view of such large inconsistencies in the test data, a high accuracy of prediction obviously cannot be expected. A summary indicative of prediction accuracy is given in Table I(b).

Reference 2 also presents the analysis of a large number of tests for static strength on sheet and bar specimens containing fatigue cracks or saw cuts as well as machined (finite-radius) notches. Since the strength of cracked parts is the area of greatest current interest, some of the results are reproduced here to illustrate key points (figs. 8 to 11). In a few test sets, separate measurements were made for longitudinal and transverse specimens (with-grain and cross-grain); in such cases, the results were averaged for presentation here.

Figure 8 shows plots of net-section stress at failure (based on net section at beginning of test) versus the ratio of crack length to specimen width for the widest sheet specimens tested ($w = 35$ in.). Figure 9 shows similar plots for the narrowest specimens tested ($w = 2.25$ in.). The specimens had either fatigue cracks or jeweler's saw cuts intended to simulate fatigue cracks. For the latter, calculations were made on the basis of two bracketing assumptions; one assumption was that the saw cut terminated with mathematically square corners ($\rho = 0$), the other one that the saw cut terminated with a semicircle (ρ equal to half-width of cut).

For the wide specimens discussed in reference 2 ($w = 35$, 20, 12, and 9 inches), there were almost no coupon tests of material properties; calculations were therefore based on typical material properties (E, e, σ_u) as given by reference 5. A correction for buckling was applied to the strength predictions where necessary. (See appendix.)

Examination of all the results presented in reference 2 showed considerable scatter for the strongest alloy tested (zinc-alloy 7075), resulting in a considerable percentage of unconservative predictions. A second set of calculations was therefore made for this alloy, using minimum elongation rather than typical. On this basis, there were no unconservative predictions, but naturally a few quite conservative ones. With this exception, there was, in general, reasonably satisfactory agreement between prediction and test for all alloys and all widths.

It was widely believed at one time that a jeweler's saw cut simulates a fatigue crack with an accuracy sufficient for engineering purposes. Examination

of figure 9 shows that this belief is marginally acceptable for 2024 alloy, but not for 7075 alloy.

Comparison of the net-section stresses developed at a given ratio 2a/w by the wide specimens (fig. 8) and the corresponding stresses developed by the narrow specimens (fig. 9) shows that the latter are two to three times larger than the former. This is an unavoidable consequence of the size effect. For the 2024 alloy specimens, the net-section stress is equal to or more than the yield stress; the specimens are thus somewhat beyond the limit of strict applicability of equation (4). It is obvious that a specimen width of 1 inch (which has been widely used for screening tests) would be undesirable for most aluminum alloys.

Results shown in reference 2 for the two weakest aluminum alloys tested (σ_u = 35 and 38 ksi) indicate that the predictions tend to become conservative for such weak alloys. It may be noted that alloys of these types are not normally used for aircraft structures and that their manufacturing control is not as close as for aircraft materials. There is circumstantial evidence that the largest discrepancy between test and prediction may have been caused partly by the particular sheet used for the tests having substantially better properties than the typical properties used in the predictions.

There exists at present considerable uncertainty on the effects of thickness of specimen and of geometric parameters such as ratio of net-section width to thickness and ratio of thickness to notch radius. For aluminum-alloy parts containing cracks, the test data and predictions shown in figures 10 and 11 for plate and bar specimens appear to justify the tentative conclusion that the method of analysis presented in this paper may be usable for thicknesses up to about 3/4 inch. Noteworthy is the fact that the specimens shown in figure 11 have ratios of net-section width to thickness as low as 0.4, proportions which are usually believed to require the consideration of biaxiality effects. For parts containing finite-radius notches, the situation is much more complex and requires more investigations.

The tentative conclusion that the method of crack analysis may be applicable to thicknesses up to 3/4 inch should not be considered as valid for other materials without special investigations. In some cases - for instance steel sheet with a decarburized skin - a strong effect of thickness should obviously be expected when dealing with very thin sheet.

All tests discussed so far were room-temperature tests. Figure 12 shows the results of an investigation on aluminum-alloy sheets extending from room temperature to -320° F (ref. 6). Plotted are tensile strengths, elongations, and notch-strength ratios (NSR), defined as the ratio of notch strength to tensile ultimate strength. The notch strength is defined as the stress at maximum load, based on the original net section of a Vee-notch specimen; the dimensions of the specimen are given in the legend of the figure. The figure shows experimental points for the NSR and calculated (full-line) curves, based on the experimental values of tensile strength and elongation. The agreement is poorest again for the zinc-alloy (7075) (fig. 12(b)), but the disagreement is well within the bounds considered to be inherent in the prediction method at its present stage of development.

The agreement for the weakest alloy (6061) with a room-temperature strength of 46 ksi is quite good in this test series. It may be noted that the NSR of all the aluminum alloys tested is fairly constant with temperature.

Static Notch Strength of Titanium Alloys

The application of the notch-analysis method to titanium alloys has been attempted only recently - within the past year. The testing of titanium alloys has been pursued very actively during the past few years, but as noted before, sharp differences sometimes exist between results obtained under nominally identical conditions, presumably due to variability of the material, variability of its response to heat treatment or differences in interstitial elements. Moreover, much of the work is still exploratory, covering a large field with a minimum number of specimens. A large volume of test data has been analyzed, but the presentation here is confined to sets of data which involve cryogenic as well as elevated test temperatures.

As in the case of the aluminum alloys, some tests were made for longitudinal and transverse grain direction separately, but were averaged for presentation here.

As first example, figure 13 shows test results on six titanium alloys which are counterparts to the results on aluminum alloys shown in figure 12, having been obtained in the same investigation (ref. 6). All titanium alloys show drastic increases in tensile strength as the temperature decreases; partly as a result of this increase, most alloys show substantial to drastic decreases in notch-strength ratio (NSR) with temperature. The agreement between experimental and calculated NSR varies from fair to poor at cryogenic temperatures. It should be noted that, in general, elongation values at room temperature were the averages of two tests, while elongation values at all cryogenic temperatures were based on a single test; the reliability of the elongation values at low temperatures is therefore questionable. Discrepancies between predictions and tests as large as those shown for the first alloy in figure 13(a) (Ti 7Al-4Mo) would call for further tests if this alloy is still considered important.

Figure 14 shows a similar plot, but based on a compilation of data obtained in a large-scale screening program to obtain data on materials of interest for a supersonic transport (ref. 7). The test data shown in figure 14 are average values shown on a summary plot in the reference. The agreement between test and calculation is rather good for these tests at all temperatures (-110° F to +650° F). The better agreement - as compared with that shown in figure 13 - is tentatively attributed to the higher statistical reliability of the data.

Figure 15 shows results on 8-inch-wide sheet specimens with fatigue cracks, obtained at the NASA Langley Research Center. This type of specimen has been recommended for the purpose of obtaining design data, because it will give more accurate and more reliable data than the 1-inch-wide Vee-notch specimens used for screening tests. The results are plotted in the form of notch strengths (net-section stresses) rather than ratios in order to avoid confusion with the notch-strength ratios currently quoted, which are usually based on 1-inch-wide Vee-notch specimens.

For two of the materials shown (figs. 15(a) and 15(b)), the notch strength varies but little over the temperature range of the tests (-110° F to +550° F). For the third material (α-alloy) (fig. 15(c)), the notch strength at 550° F is markedly higher than at room temperature or at -110° F. The scatter is reasonably small, and the agreement with the prediction is reasonably good with the exception of 6Al-4V alloy at 550° F.

Rate of Propagation of Fatigue Cracks

For the purpose of chosing inspection intervals for aircraft in service, there is great interest in the problem of estimating the rates at which fatigue cracks propagate.

In reference 8, extensive measurements of propagation rates on two aluminum alloys were plotted against the product $K_N S_N$, which is a measure of the (effective) stress at the tip of the crack. (The quantity K_N in ref. 8 corresponds to K_{TN} of the present report, but is computed by a somewhat different method and with different values of ρ'.) It was shown that the measured propagation rates fell into a reasonably narrow band on these plots; thus, a curve fitted to the results can be used to predict the propagation rates.

Although, as noted, the K_N of reference 8 is not identical with the K_{TN} of the present report, a conversion can be made, and the propagation rates could be plotted against $K_{TN} S_N$ with similar results. For future applications to other materials, it should be noted that the method of reference 8 involves two constants for each material (ρ' and ρ_e) instead of the single constant ρ' required by the method of the present paper; the simultaneous determination of the two constants is difficult in practice.

SPECIAL APPLICATIONS

Correlation of Results From Different Types of Specimens

Notch tests have been conducted in the past using a large variety of specimen shapes and sizes. Recently, some standards have been recommended (refs. 9(a) and 9(b)). However, these proposed standards are not sufficiently definite in some respects, as the following detailed analysis will demonstrate. On the other hand, it appears very doubtful that a single rigid standard can be found which will meet the greatly differing requirements for purposes such as materials research, production and processing control, acceptance testing, and provision of design data. Thus, there will be a continuing and frequent need for comparing results obtained on different types of specimens. The following sample application will demonstrate how notch analysis can be used as a tool for rational comparisons.

Although it is generally recognized that the ideal "notch" for fracture-toughness tests is a crack, many investigators still use Vee-notches with a

finite radius. Reference 9(c) reports results of tests in which notch radius was the main variable, with the crack ($\rho = 0$) included as basic standard. Minor variables were specimen width and method of machining the notch radius. Figure 16 shows plots of the test results. (In ref. 9(c), the ordinate was K_c rather than notch-strength ratio; the differences between the two types of plots are negligible, and an approximate scale of K_c is shown on the right-hand edge of fig. 16(a).) The empirical analysis made in reference 9(c) consisted in drawing a horizontal line through point A in figure 16(a) (average of tests on specimens with cracks) and a sloping line (dash-dot) through the test points for radiused specimens. The intersection of these lines was interpreted to define the maximum radius $(0.25 \times 10^{-3}$ inch) which could be expected to simulate a crack. The standards proposed in references 9(a) and 9(b) specified the radius as "1×10^{-3} inch maximum." Thus, even the brief empirical analysis of reference 9(c) showed that the proposed standard was too loose for tests on this type of material.

The notch-analysis method of the present paper has now been applied to these data as follows. The Neuber constant ρ' was computed from the notch-strength ratio at point A, figure 16(a). The tensile strength was estimated from comparison tests (about 310 ksi). The elongation was not reported. For a similar heat treatment, reference 10 gave $e = 9$ percent; computations were therefore made assuming $e = 8$ percent and $e = 10$ percent. With these data, the notch-strength ratios were computed as shown by the curves in figure 16 for the 1-inch as well as the 3-inch specimens.

Inspection of figure 16(a) shows that the test points for radii of 2, 3, and 4×10^{-3} inch lie very close to the computed curves. Thus, these tests correlate perfectly with the results on the cracked specimens (point A). Results for specimens with a radius of 1×10^{-3} inch lie somewhat below the curve; thus the correlation would not be quite so good. The tests results for specimens with $\rho = 0.6 \times 10^{-3}$ inch show large scatter, and their average lies so far below the curve that the correlation is extremely poor.

Thus, although the notch-strength ratios of the specimens with radii of 2, 3, and 4×10^{-3} inch are three to four times larger than for cracked specimens, the results can be used successfully to compute the strength of the cracked specimen by means of notch analysis. By contrast, the "fracture-mechanics" procedures outlined in reference 9(a) can only state that a radius is either small enough to simulate a crack satisfactorily, or that it is too large for satisfactory simulation.

It was mentioned previously that the empirical analysis of figure 16(a) resulted in the conclusion that the notch radius should be less than 0.25×10^{-3} inch to simulate a crack. Although cautiously phrased, this conclusion appears to be questionable in the light of the notch analysis. The calculated curves predict, in effect, that a well-machined specimen with a radius of 0.25×10^{-3} inch would have a notch strength twice as high as the crack which it is intended to simulate.

Turning now to the results for 3-inch specimens (figs. 16(b) and 16(c)), it may be noted that the computed curves pass precisely through the experimental points for cracked specimens ($\rho = 0$). Thus, notch analysis predicts accurately the substantial drop ($\approx$33 percent) of cracked strength which is the result of increasing the specimen width from 1 inch to 3 inches.

For 3-inch specimens with finite radii, the agreement with prediction is again very poor for notch radii of 0.6×10^{-3} inch. For radii of 1×10^{-3} inch, the agreement is good for center slots but very poor for edge notches. Since theory and many tests agree that center slots and edge notches should give essentially the same results, the tests must be judged unreliable.

A reasonable over-all conclusion would be that tests on specimens with notch radii of 2×10^{-3} inch or greater can be correlated very well with tests on cracked specimens; width effects can also be predicted very well. For notch radii of 1×10^{-3} inch or less, however, the correlation is marginal to very poor. Two possible reasons may be suggested: either the radii are inaccurate, or the roughness of elox cutting (electric-discharge cutting) becomes important at such small radii.

Criteria for Comparison of Materials

When a preliminary choice of materials is being made for a new design, it is useful to have criteria which describe important characteristics of the material in numerical form, preferably by a single number in order to make comparisons simple. The two characteristics to be discussed here are fatigue notch sensitivity and static notch sensitivity.

Consider two parts made of different materials, but having identical notched configurations and thus identical values of K_T. The fatigue factor is calculated from K_T by formula (3), which contains only one materials constant, the Neuber constant ρ'. Thus, ρ' can be used directly as criterion for fatigue notch sensitivity, bearing in mind that the sensitivity increases as ρ' decreases. It should be noted that this criterion measures only sensitivity to high-cycle fatigue; when low-cycle fatigue is of concern (say $N < 10{,}000$), a different criterion is needed.

To arrive at a simple criterion for static notch sensitivity, a "standard configuration" must be selected. A suitable choice appears to be an infinitely wide (sheet) specimen with a "central" transverse slit. Although an infinitely wide sheet cannot be tested in a laboratory, it is a convenient reference basis also used in fracture mechanics (ref. 9(a)).

Concerning notch radius, it seems desirable to adopt the limiting case of vanishing radius - the crack - as standard. Any finite radius would be completely arbitrary. Moreover, service problems are encountered mostly as result of fatigue or welding cracks, not as results of small-radius notches.

Finally, the crack length must be specified. When this is done, the number which measures the notch sensitivity is the stress which causes failure. However, the inverse is also possible: a standard stress level for failure may be specified, and the characteristic "yardstick" number which results then is a crack length.

The first method has been chosen - in effect - in "fracture mechanics" (ref. 9(a)). The quantity K_c used to describe the notch sensitivity may be defined as being numerically equal to the failing stress in an infinitely wide sheet containing a crack with a length $2/\pi$. (To be consistent with numbers conventionally quoted, the stress must be measured in ksi, and the crack length in inches.)

With the theory of the present report, the quantity K_c can be calculated in two steps by the formulas

$$K_u = 1 + \frac{2}{\left(1 + \frac{0.8eE}{\sigma_u}\right)\sqrt{\pi\rho'}} \tag{8a}$$

$$K_c = \frac{\sigma_u}{K_u} \tag{8b}$$

It should be noted that the present theory is based on the use of initial crack length, while K_c measurements are supposed to be based on the crack length existing at the instant when the crack becomes fast running. (In practice, this specification is not always followed.) Thus, direct comparisons between values calculated by formulas (8a) and (8b) and reported values of K_c are permissible only if there is no slow cracking, or if the investigator elected to base his K_c calculations on initial crack length.

For the second method specifying a standard stress level, the suggestion has been made by P. Denke to use as comparison number the crack length in an infinitely wide sheet which reduces the strength to one-half of the strength of the uncracked sheet. This suggestion amounts to using $K_u = 2$ as standard case; formulas (4), (6), and (7) yield for the characteristic crack length

$$(2a)_{0.5} = \frac{1}{2}\rho'\left(1 + \frac{0.8eE}{\sigma_u}\right)^2 \tag{9}$$

The subscript 0.5 indicates the fractional strength level chosen as basis.

The choice of the 0.5 level was based essentially on convenience. A more rational choice might be based on the consideration that civil airworthiness requirements stipulate that a cracked structure should have a strength equal to 2/3 of the strength of the undamaged structures. To correlate with this requirement, a factor $K_u = 1.5$ would be chosen; the corresponding crack length in the

infinitely wide sheet would then be

$$(2a)_{0.67} = \frac{1}{8}\rho'\left(1 + \frac{0.8eE}{\sigma_u}\right)^2 \qquad (10)$$

or one-fourth of the value given by expression (9).

Material properties and values of $(2a)_{0.5}$ are given in the tabulation below for two principal aluminum alloys used for aircraft skins, for the thickness range from 0.021 to 0.249 inch.

	E, ksi	σ_u, ksi	e, percent	ρ', in.	$(2a)_{0.5}$, in.
2024-T3	10.6×10^3	70	18	0.0204	5.30
7075-T6	10.4×10^3	83	11	.0159	1.14
7075-T6			7		.51

The elongations of 18 and 11 percent, respectively, are typical values as listed in reference 5, as are the tensile ultimates given in the tabulation. The elongation of 7 percent is the minimum value given in reference 5. As mentioned in the discussion of notch strengths of wrought aluminum alloys, unconservative predictions for a substantial percentage of the tests (over 50 percent) resulted for 7075-T6 alloy if the typical elongation was used, and the minimum elongation had to be used to eliminate unconservative predictions. Consequently for a realistic comparison between 7075-T6 and 2024-T3, the $(2a)_{0.5}$ value for the former should be taken as closer to 0.51 inch rather than 1.14 inch. Even the larger value 1.14 inch is very much less than the corresponding value of 5.30 inch for the 2024-T3 alloy, indicating a much greater static notch sensitivity.

CONCLUDING REMARKS

The method of notch analysis for aluminum alloys presented a year ago has been greatly expanded in scope in two respects: it has been applied to titanium alloys, and it has been applied over a temperature range of about 1000° F without introducing new concepts or constants.

The number of serious discrepancies between test and prediction encountered in the analysis of individual tests on titanium has been larger than on aluminum. Since a very reasonable accuracy of prediction was achieved for statistically well-confirmed data, it is anticipated that most of the large discrepancies will be traced eventually to faulty test techniques, to factors such as interstitial elements or strain-rate effects, or to erratic behavior of the material which has not yet been overcome entirely due to the rapidity with which the technology of titanium is being developed.

The method has not yet been applied on a large scale to the analysis of notch sensitivity of materials such as stainless steels and superalloys. However, the method can be applied on an individual basis, and sample applications have shown that it can be very useful for understanding notch effects, for correlating tests performed on different types of specimens, and for reducing or eliminating costly and uncertain empiricism in the choice of test specimens.

APPENDIX

Buckling Correction

A sheet with a transverse slot (fig. 2(b) or 2(d)) will tend to buckle along the slot when the sheet is subjected to tensile load; the buckling deformation lowers the strength of the sheet. In order to allow for this effect, the strength of the sheet as predicted on the basis of the failure criterion (1a) or (1b) should be multiplied by the empirical factor

$$\left(1 - 0.001\frac{2a}{t}\right) \tag{A1}$$

where $2a$ is the total slot length and t is the thickness of the sheet (ref. 2).

Formula (A1) is based on a very small number of tests and consequently of questionable reliability. It is suggested, therefore, that buckling be suppressed by guide plates if feasible when the buckling effect exceeds some chosen percentage, say 5 percent or 10 percent ($2a/t = 50$ or 100, respectively).

The buckling correction should not be applied when the curvature correction of the following section is applied.

Curvature Correction

Experience has shown that the factor K_u is considerably larger for a longitudinal slot in a cylinder under internal pressure than for a corresponding flat sheet. An empirical correction factor for aluminum alloys is

$$K_{uCYL} = K_{uFLAT}\left(1 + 5 \times \frac{2a}{R}\right) \tag{A2}$$

where $2a$ is the total length of the longitudinal slot and R is the radius of the cylinder (ref. 11).

In reference 11, an older method was used to calculate the factors for flat sheets. Use of the method given in the present paper resulted in a factor 5 as given above instead of the factor 4.6 given in reference 11.

REFERENCES

1. Kuhn, Paul, and Hardrath, Herbert F.: An Engineering Method for Estimating Notch-Size Effect in Fatigue Tests on Steel. NACA TN 2805, 1952.

2. Kuhn, Paul, and Figge, I. E.: Unified Notch-Strength Analysis for Wrought Aluminum Alloys. NASA TN D-1259, 1962.

3. Dixon, J. R.: Stress Distribution Around Edge Slits in a Plate Loaded in Tension. J. Roy. Aero. Soc., May 1962.

4. Herrnstein, William H., III, and McEvily, Arthur J., Jr.: Effects of Decarburization on Notch Sensitivity and Fatigue-Crack-Propagation Rates in 12 MoV Stainless-Steel Sheet. NASA TN D-966, 1961.

5. Anon.: Alcoa Aluminum Handbook. Aluminum Company of America, 1959.

6. Hickey, Charles F.: Mechanical Properties of Titanium and Aluminum Alloys at Cryogenic Temperatures. ASTM Preprint 78, 1962.

7. Raring, Richard H., Freeman, J. W., Schultz, J. W., and Voorhees, H. R.: Progress Report of the NASA Special Committee on Materials Research for Supersonic Transports. Part I - Committee Activities. Part II - Results of Supersonic Transport Materials Screening Program. NASA TN D-1798, 1963.

8. McEvily, Arthur J., Jr., and Illg, Walter: The Rate of Fatigue Crack Propagation in Two Aluminum Alloys. NACA TN 4394, 1958.

9. Anon.: Fracture Testing of High-Strength Sheet Materials. A Report of a Special ASTM Committee. Materials Research and Standards Bulletin, ASTM.
   (a) First Report, chapter I, January 1960.
   (b) First Report, chapter II, February 1960.
   (c) Third Report, November 1961.

10. Anon.: Properties and Selection of Materials. Metals Handbook, vol. 1, 8th edition, published by American Society for Metals, 1961.

11. Peters, Roger W., and Kuhn, Paul: Bursting Strength of Unstiffened Pressure Cylinders With Slits. NACA TN 3993, 1957.

TABLE I.- ACCURACY OF NOTCH-FATIGUE PREDICTIONS

(a) Low-alloy steels

[Data from ref. 1]

	Number of tests	Percent within ±20 percent*
Rotating beams with circumferential grooves	77	87
Rotating beams with fillets	75	92
Rotating beams with transverse holes	27	59
Axially loaded cylindrical specimen with grooves	74	81
Axially loaded sheet with notches	6	100

(b) Aluminum-alloy specimens

[Data from ref. 2]

	Number of tests	Percent within ±20 percent*
2024-T3		
Axially loaded sheet	56	84
Rotating beams	12	50
7075-T6		
Axially loaded sheet	34	85
Rotating beams	24	71
Miscellaneous alloys		
Rotating beams	34	71

*Percentage of tests for which predicted and experimental fatigue factors agreed within ±20 percent.

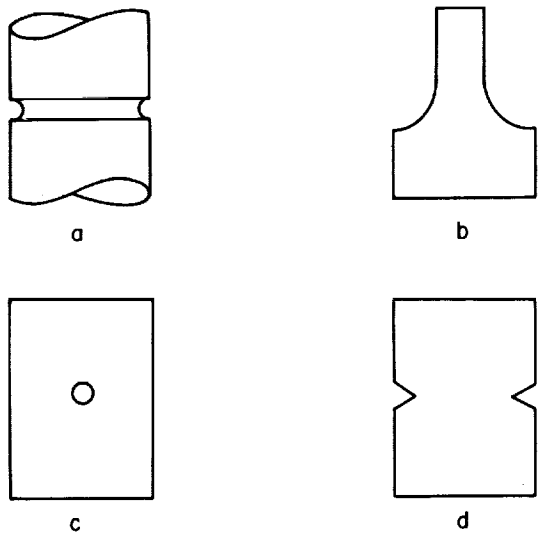

Figure 1.- Common types of notches.

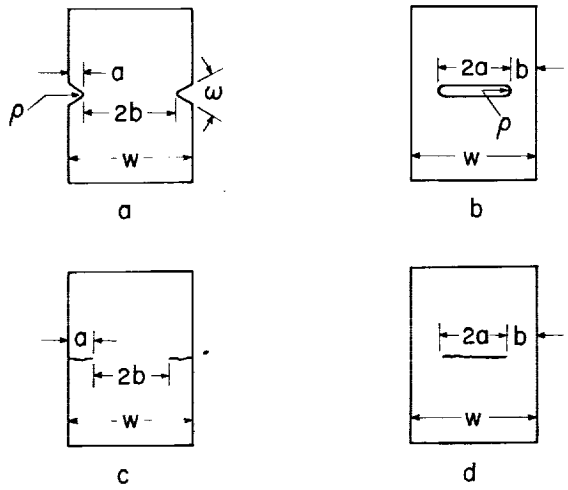

NASA

Figure 2.- Standard types of notches used in notch-sensitivity tests on sheet materials. (Uniaxial tensile loading.)

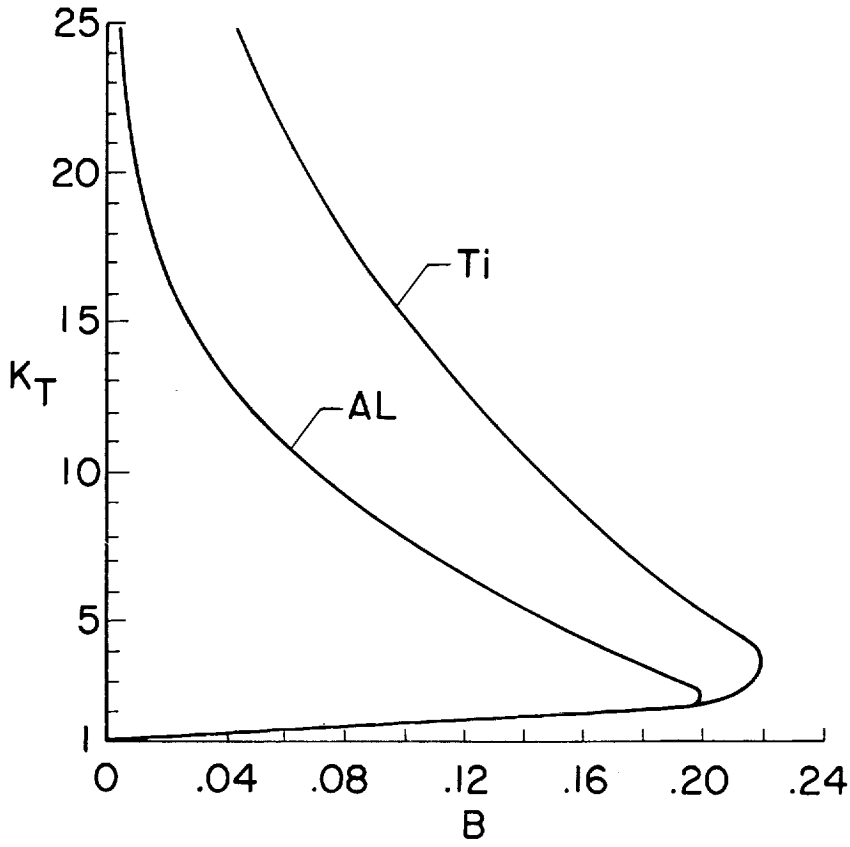

NASA

Figure 3.- Flow-restraint parameters for sheet-metal parts of aluminum or titanium alloys. (Use only when $b/t > 4$.)

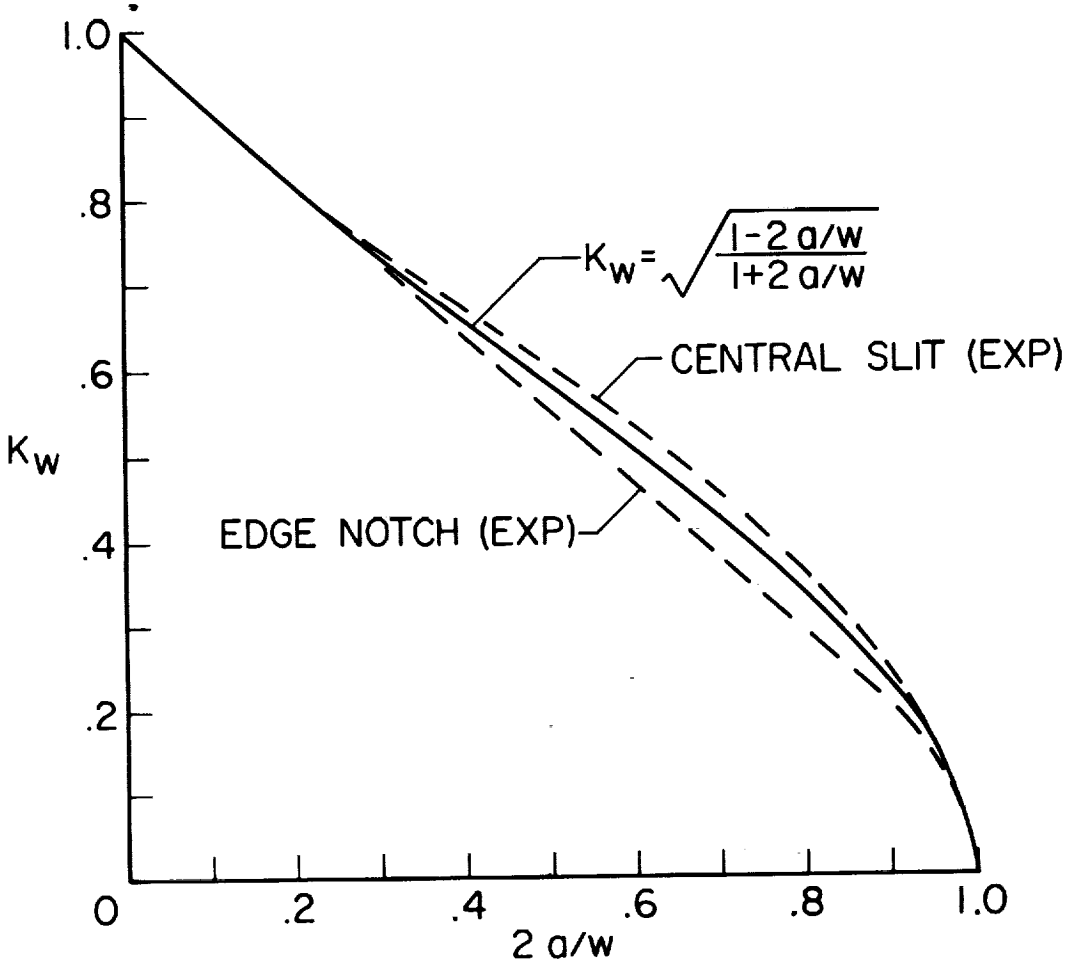

NASA

Figure 4.- Finite-width factor. (From ref. 3.)

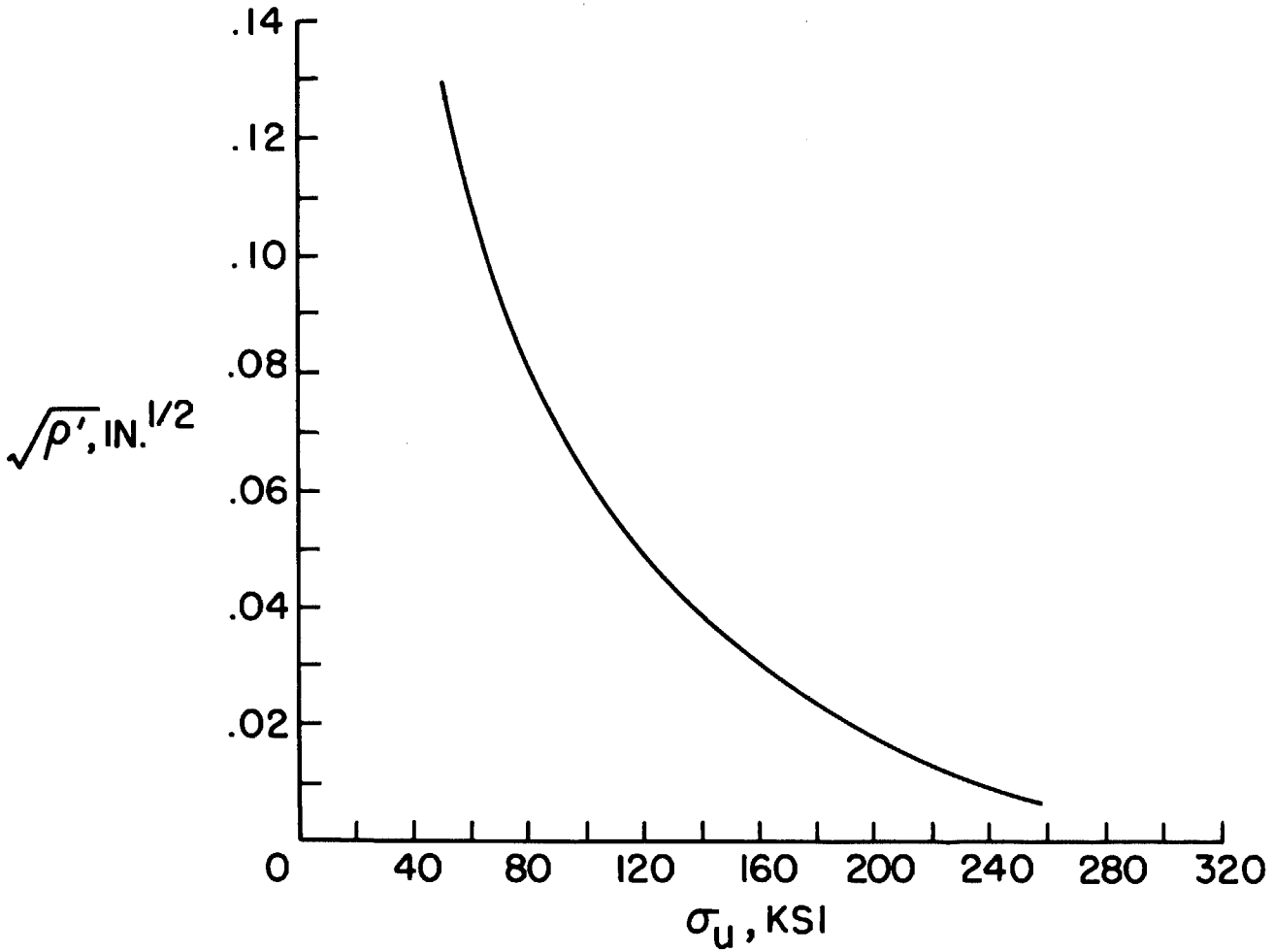

NASA

Figure 5(a).- Neuber constants for low-alloy steels. (From ref. 1.)

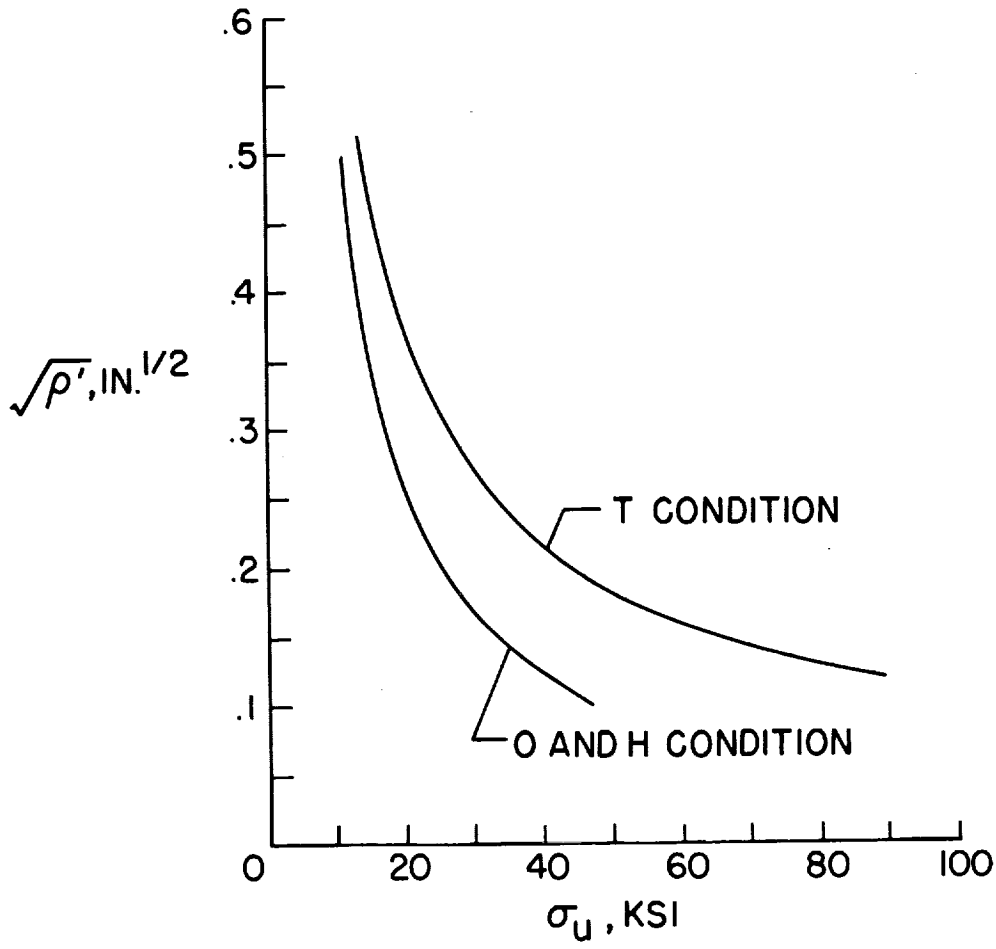

NASA

Figure 5(b).- Neuber constants for wrought aluminum alloys. (From ref. 2; T = heat-treated; O = annealed; H = strain-hardened.)

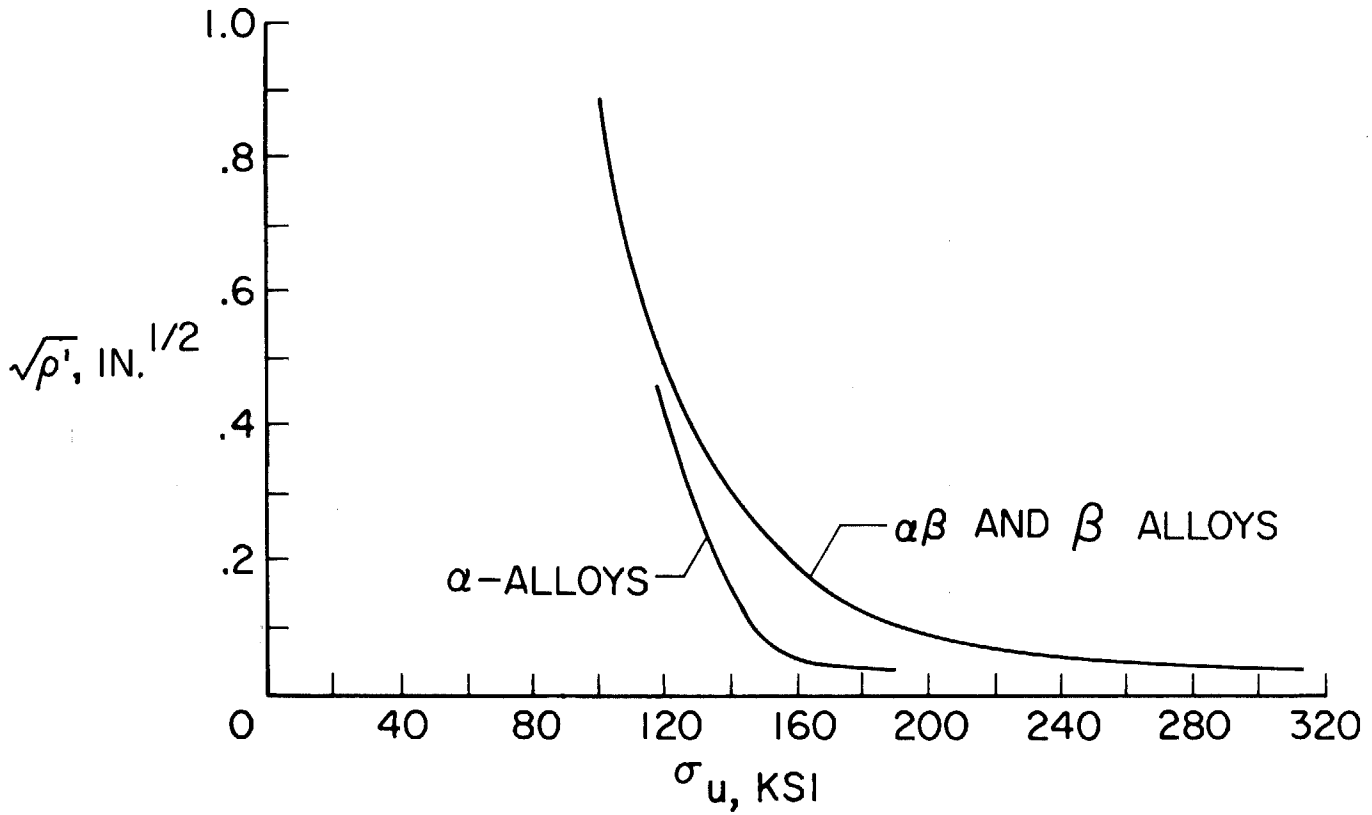

NASA

Figure 5(c).- Tentative Neuber constants for titanium alloys.

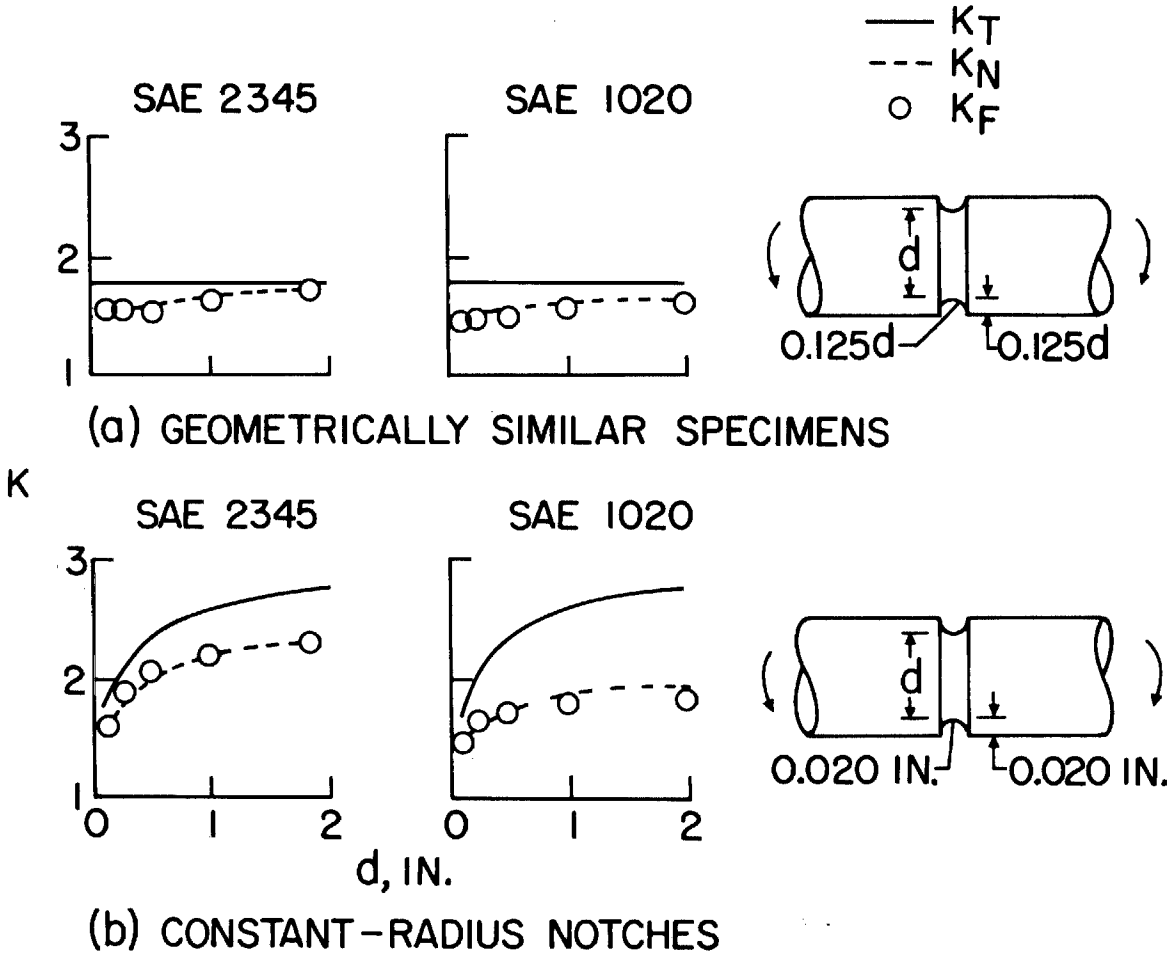

NASA

Figure 6.- Experimental and predicted notch-fatigue factors for grooved rotating beams from low-alloy steel. (From ref. 1.)

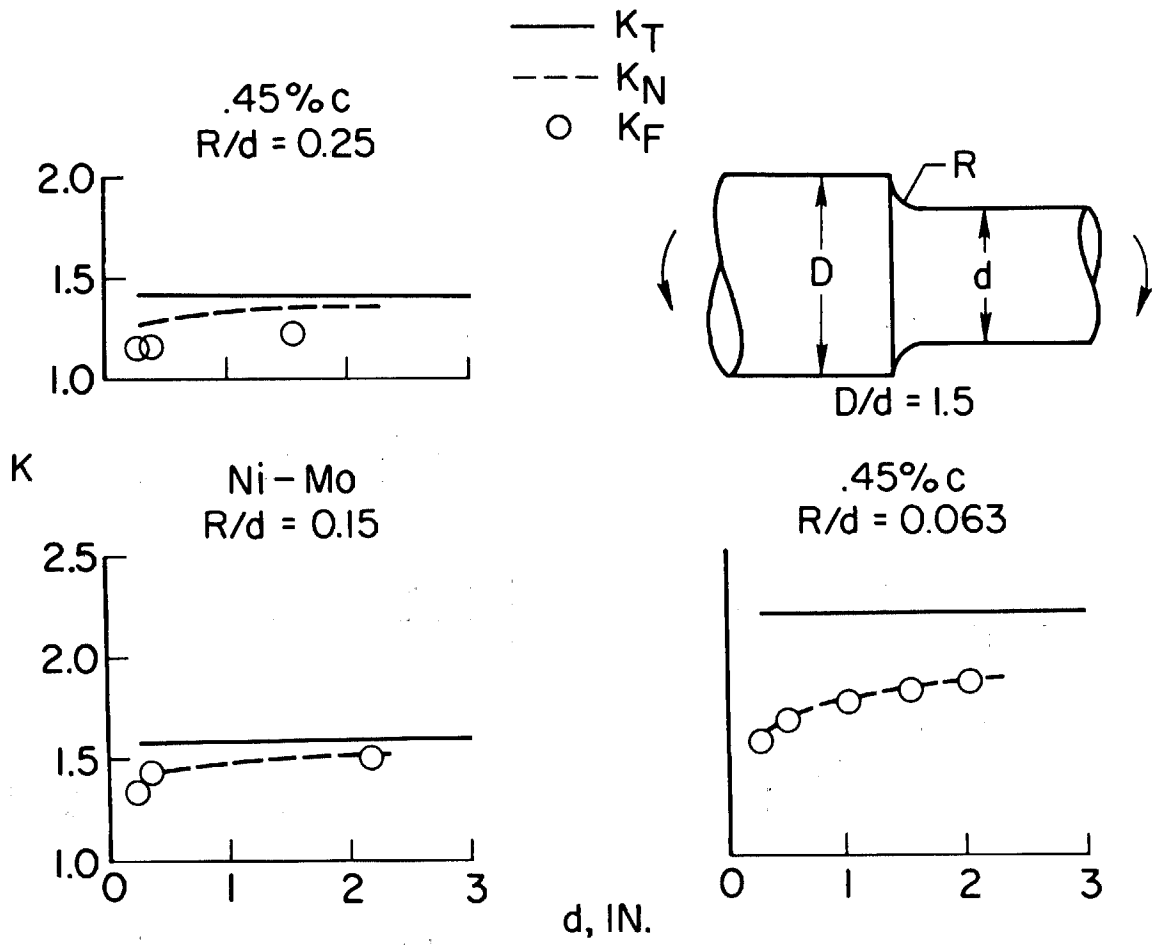

NASA

Figure 7.- Experimental and predicted notch-fatigue factors for low-alloy steel rotating beams with shoulders. (From ref. 1.)

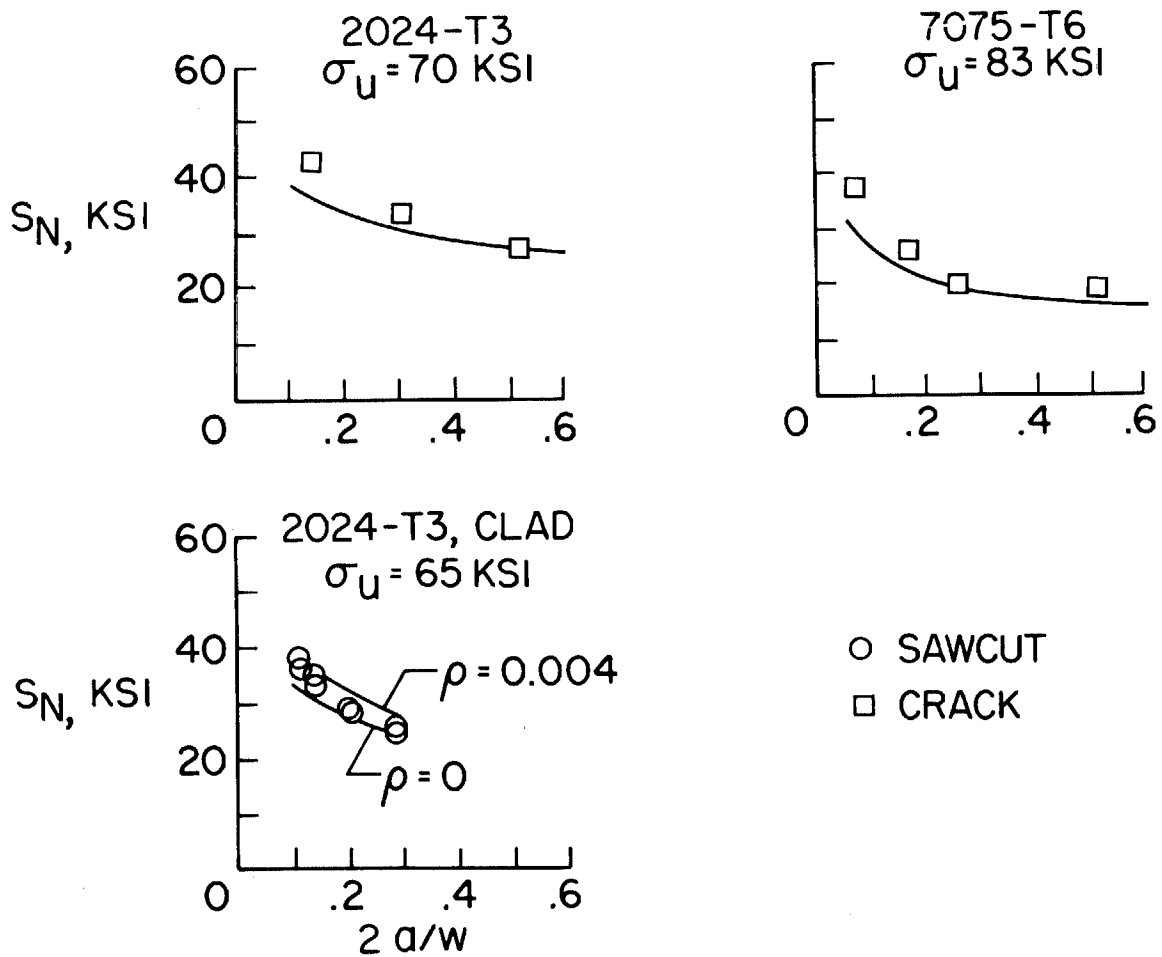

NASA

Figure 8.- Experimental and predicted failing stresses on wide aluminum-alloy sheets with center cracks or saw-cuts. (w = 35 in.; from ref. 2.)

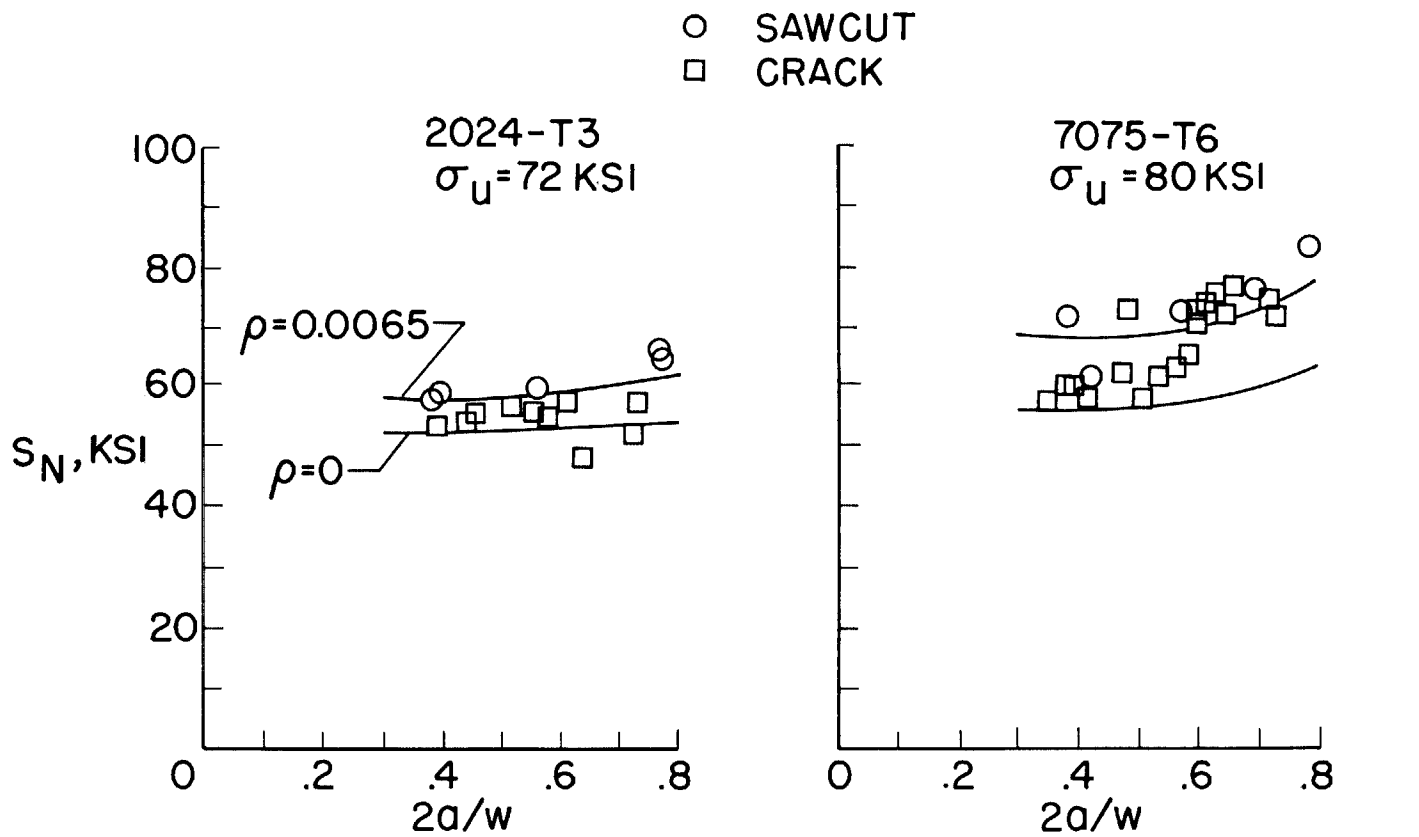

Figure 9.- Experimental and predicted failing stresses on narrow aluminum-alloy sheets with edge cracks or saw-cuts. (w = 2.25 in.; from ref. 2.)

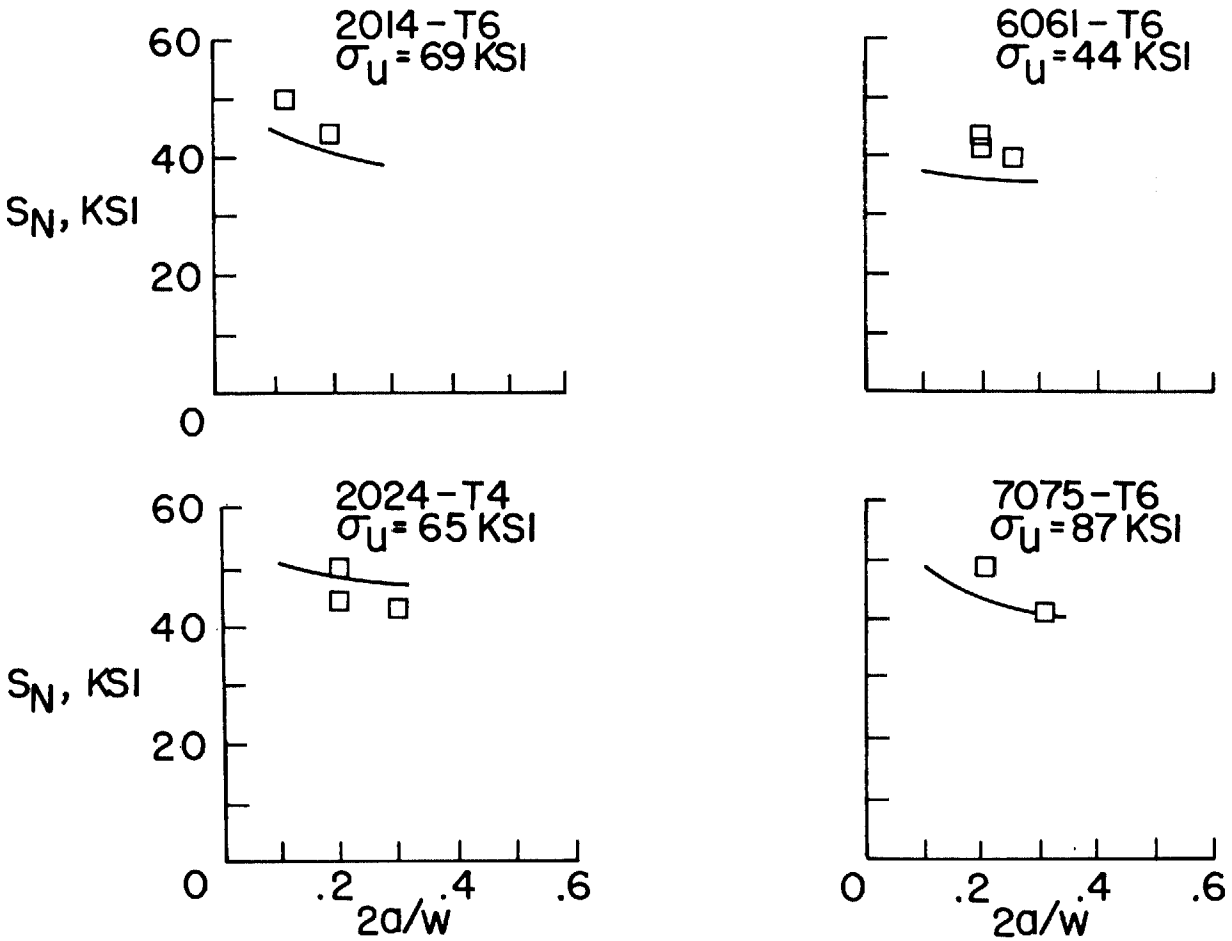

NASA

Figure 10.- Experimental and predicted failing stresses for aluminum-alloy plate with center cracks. (w = 7.5 in.; t = 0.25 in.; from ref. 2.)

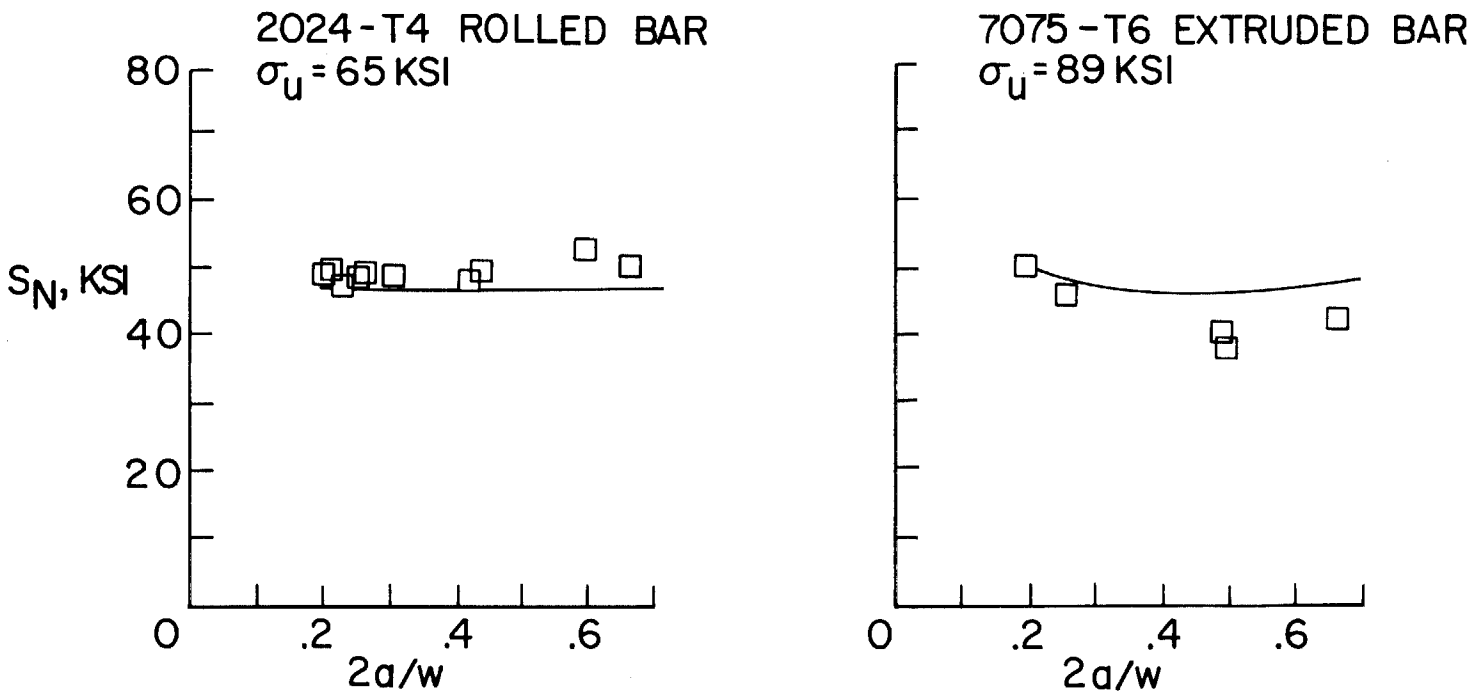

Figure 11.- Experimental and predicted failing stresses for aluminum-alloy bar with center cracks. (w = 2 in.; t = 0.75 in.; from ref. 2.)

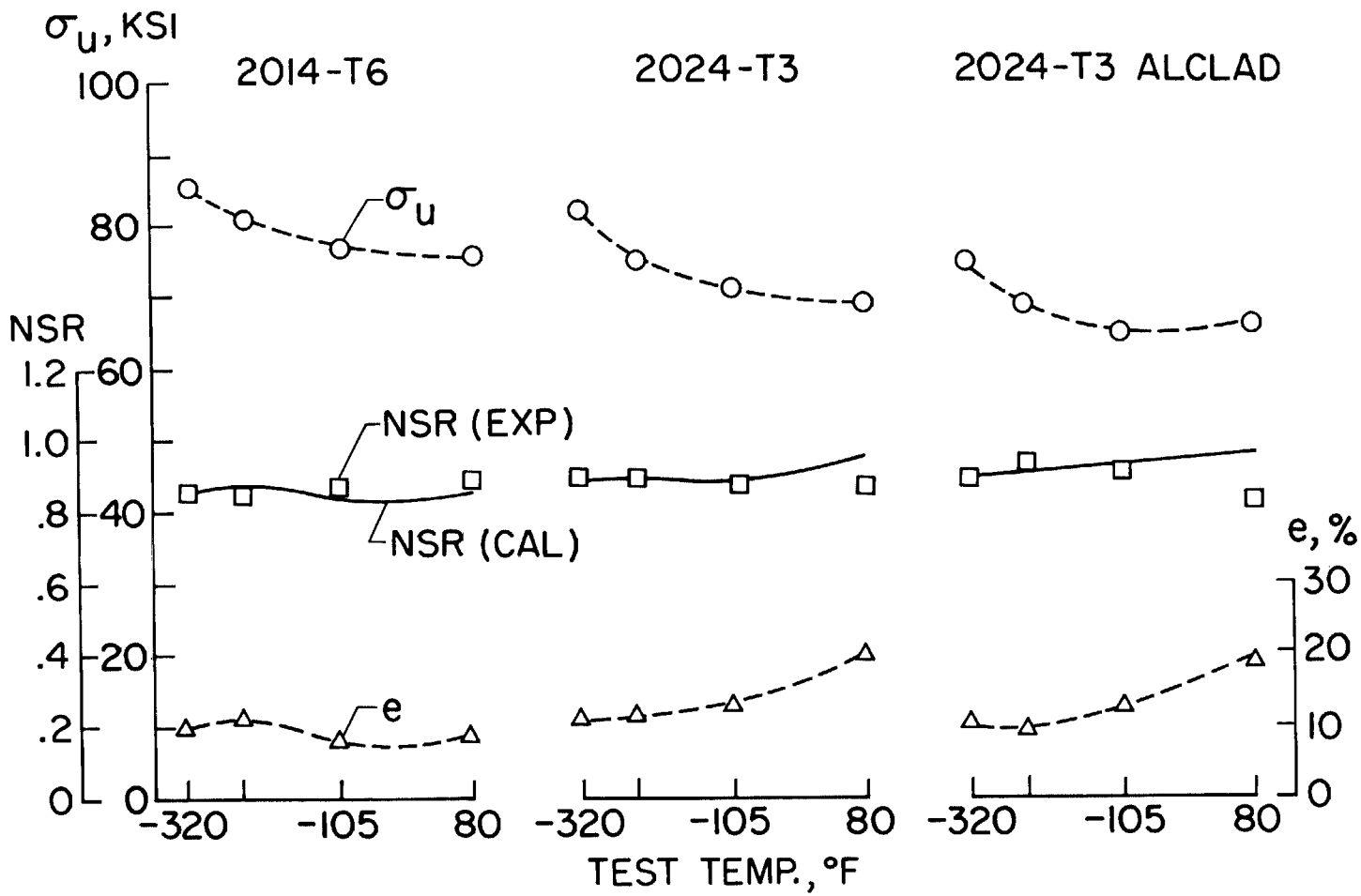

Figure 12(a).- Tensile strengths, elongations, and notch-strength ratios of aluminum-alloy sheet as function of test temperature. Full-line curves are calculated. Specimen $w \approx 0.64$ in.; 45° Vee-notch; $a \approx 0.1$ in.; $\rho \approx 0.002$ in. Data from reference 6.

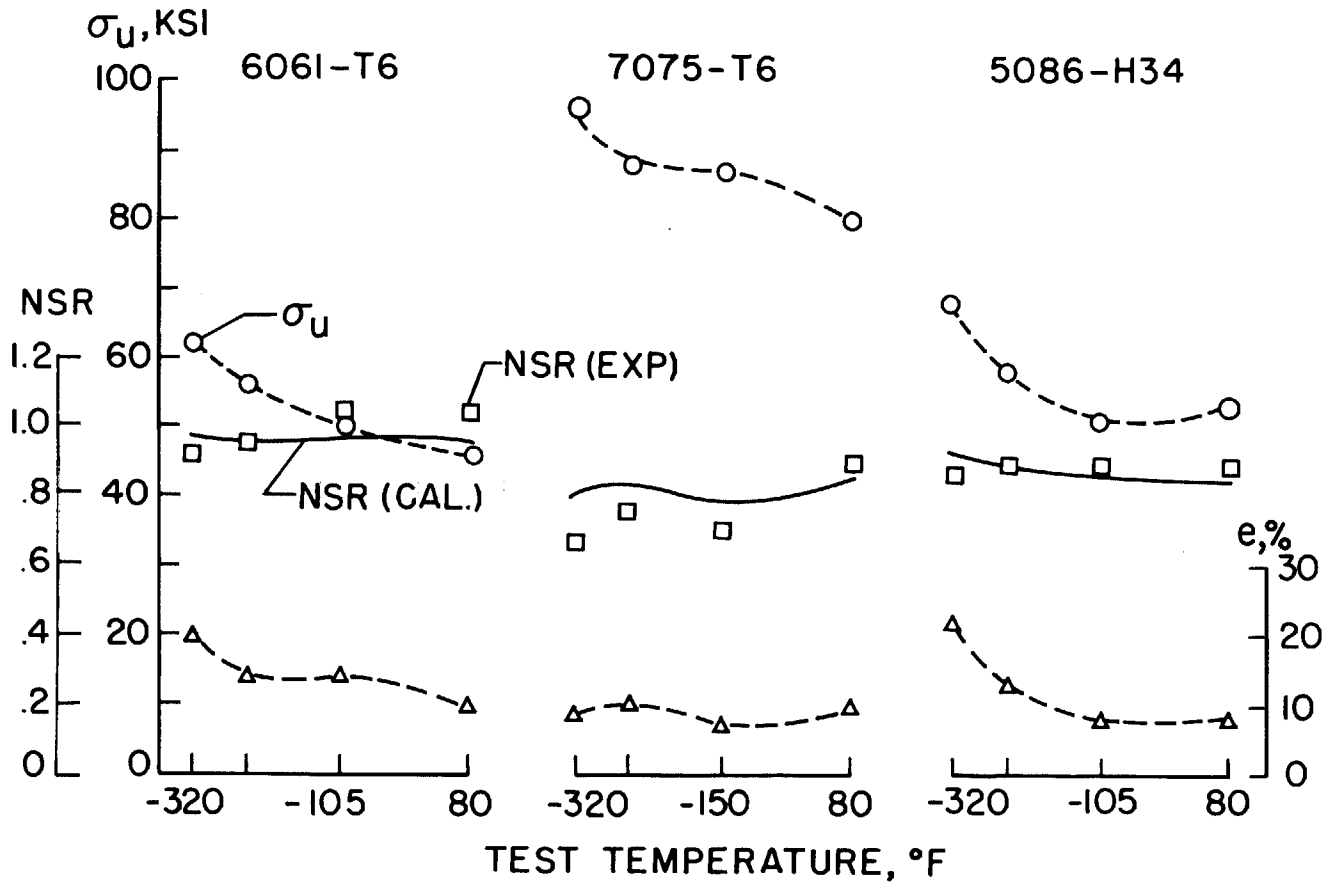

NASA

Figure 12(b).- Tensile strengths, elongations, and notch-strength ratios of aluminum-alloy sheet as function of test temperature. Full-line curves are calculated. Specimen $w \approx 0.64$ in.; 45° Vee-notch; $a \approx 0.1$ in.; $\rho = 0.002$ in. Data from reference 6.

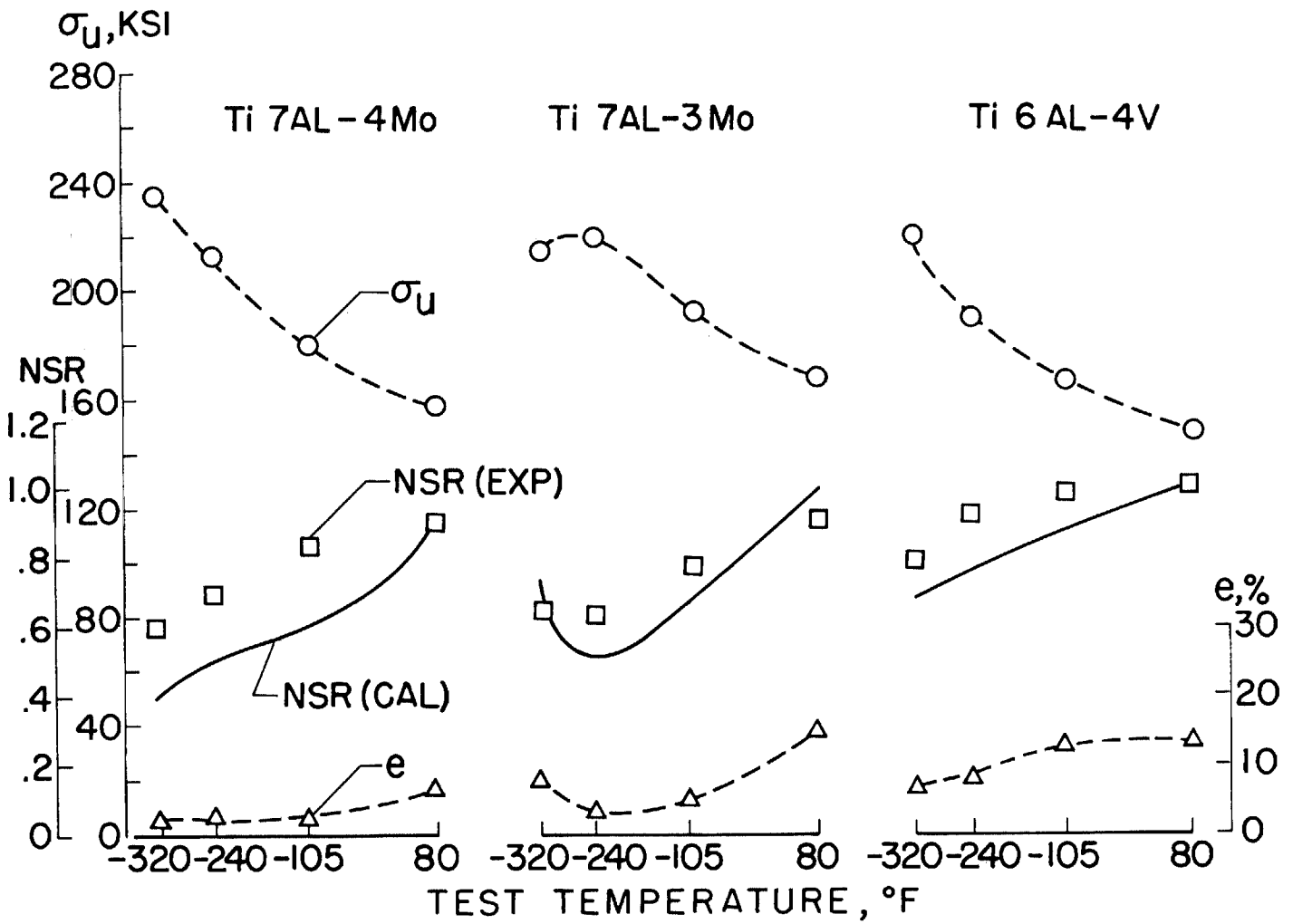

Figure 13(a).- Tensile strengths, elongations, and notch-strength ratios of titanium-alloy sheet as function of test temperature. Full-line curves are calculated. Specimen $w \approx 0.64$ in.; 45° Vee-notch; $a \approx 0.1$ in.; $\rho = 0.002$ in. Data from reference 6.

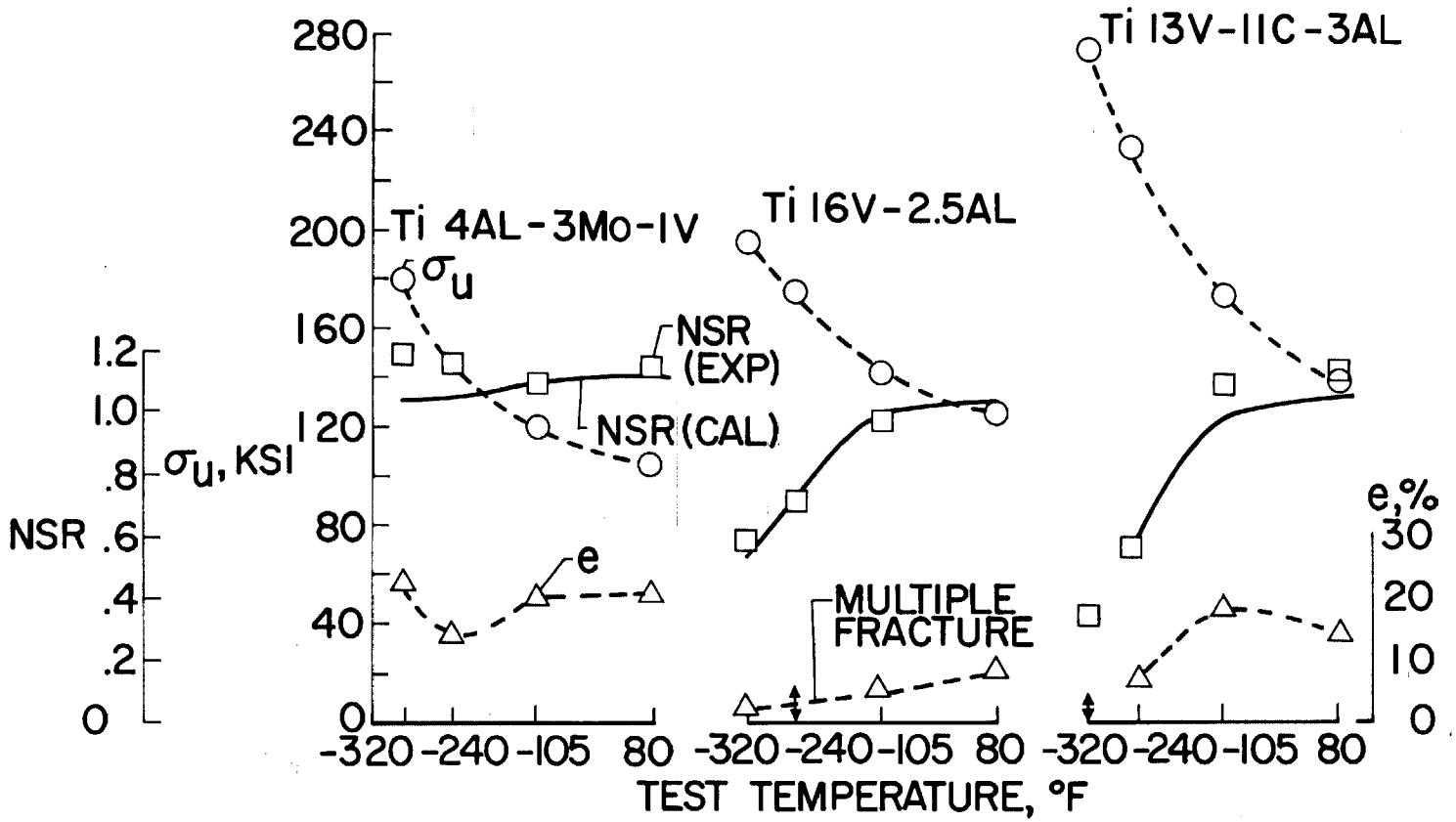

Figure 13(b).- Tensile strengths, elongations, and notch-strength ratios of titanium-alloy sheet as function of test temperature. Full-line curves are calculated. Specimen $w \approx 0.64$ in.; 45° Vee-notch; $a = 0.1$ in.; $\rho = 0.002$ in. Data from reference 6.

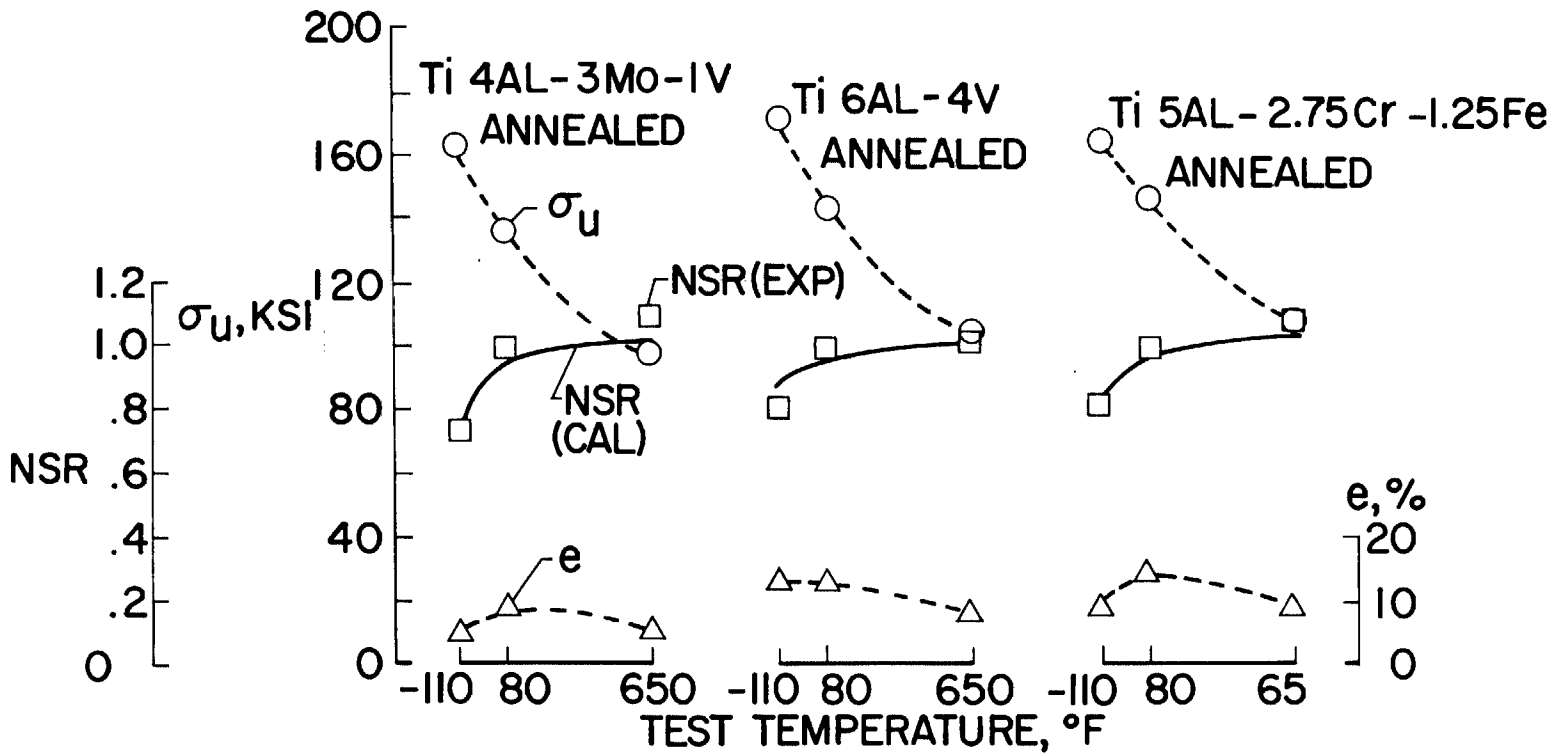

NASA

Figure 14(a).- Tensile strengths, elongations, and notch-strength ratios of titanium-alloy sheet as function of test temperature. Full-line curves are calculated. Specimen w = 1.0 in.; 60° Vee-notch; a = 0.15 in.; ρ = 0.0007 in. Data from reference 7.

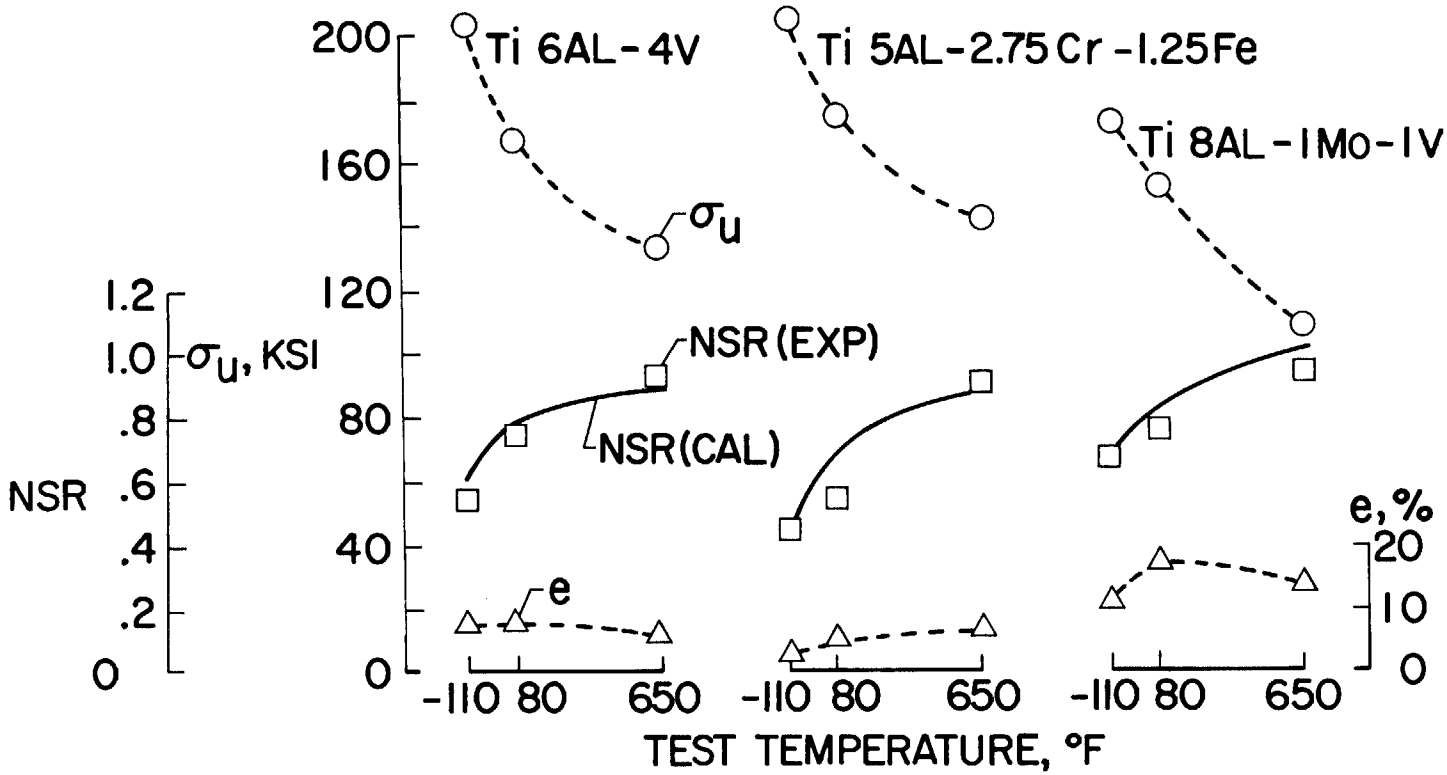

NASA

Figure 14(b).- Tensile strengths, elongations, and notch-strength ratios of titanium-alloy sheet as function of test temperature. Full-line curves are calculated. Specimen w = 1.0 in.; 60° Vee-notch; a = 0.15 in.; ρ = 0.0007 in. Data from reference 7.

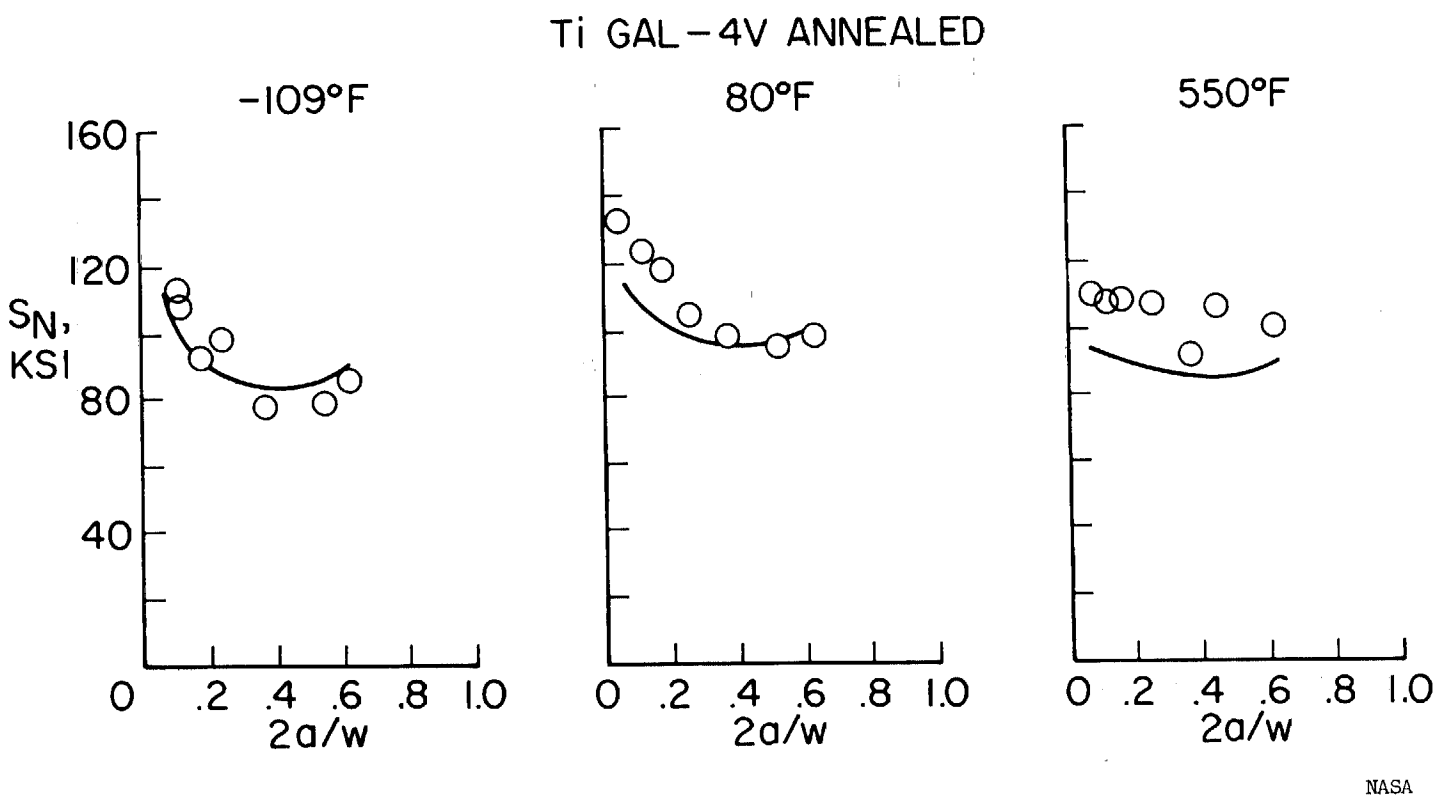

Figure 15(a).- Failing stresses for titanium-alloy sheet with center cracks. w = 8 in.; NASA data.

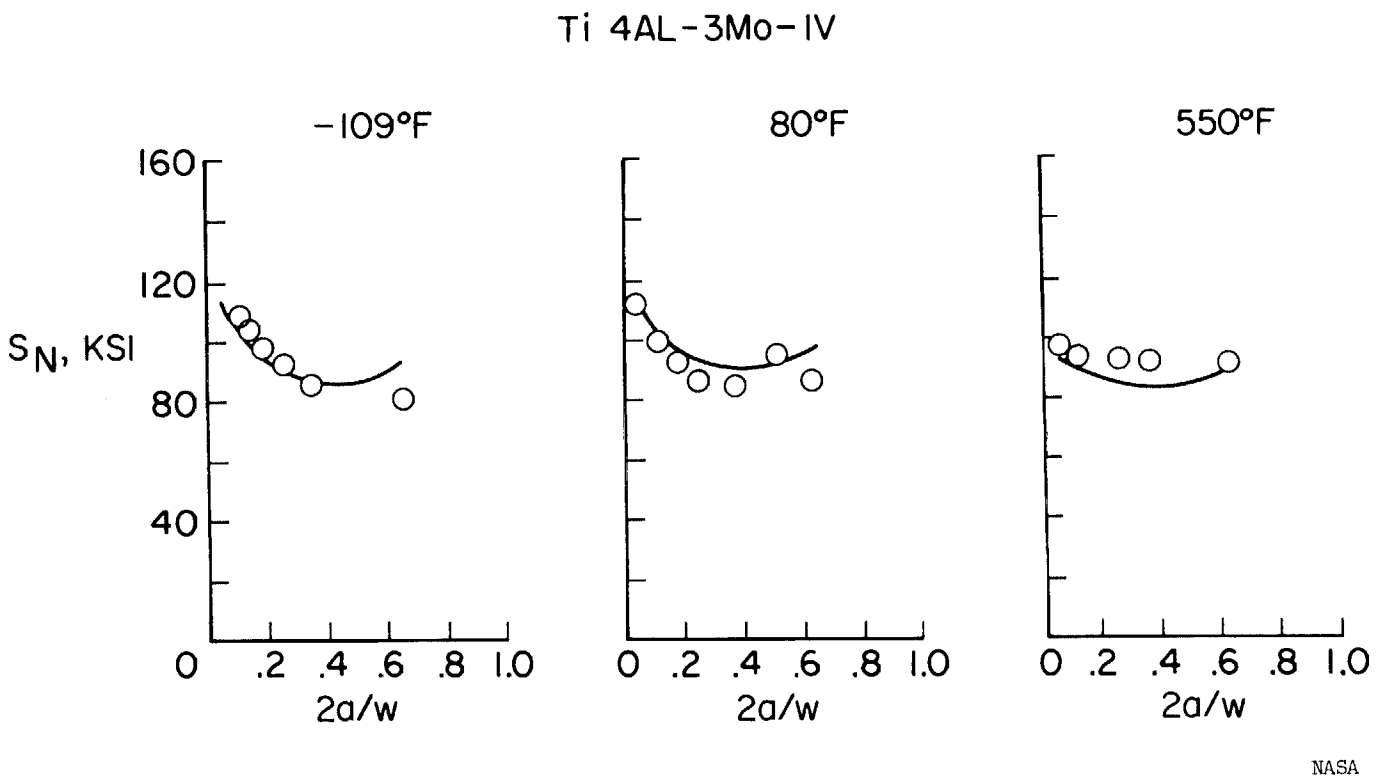

Figure 15(b).- Failing stresses for titanium-alloy sheet with center cracks. w = 8 in.; NASA data.

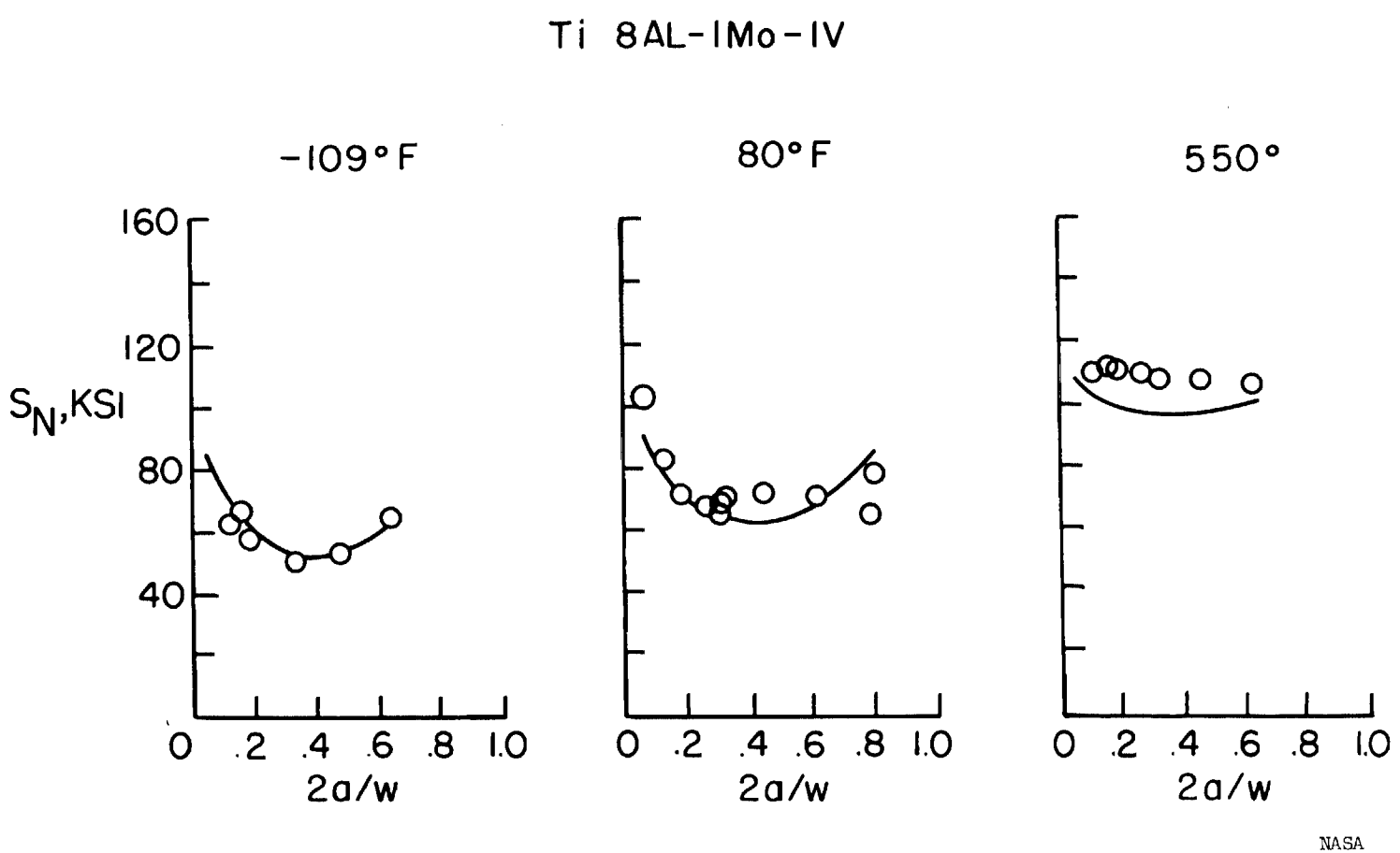

Figure 15(c).- Failing stresses for titanium-alloy sheet with center cracks. w = 8 in.; NASA data.

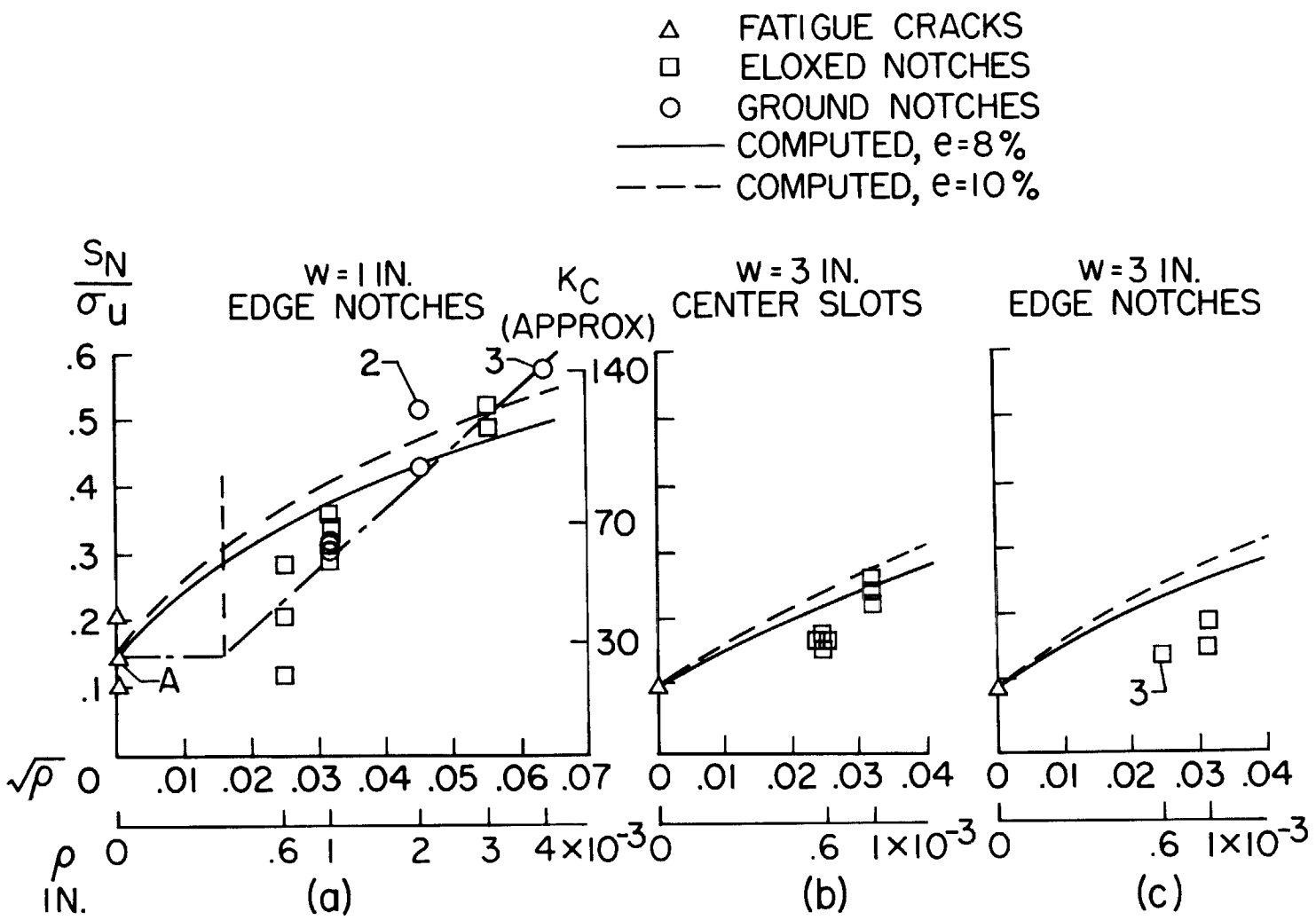

Figure 16.- Notch-strength ratio of H-11 (mod.) tool steel as function of notch radius. Data from reference 10.